



Horizon Aircraft Concept

Joint NASA/DLR Aeronautics Design Challenge 2017-2018



Team

Nils Böhnisch
René Maasmeier
René Rings
Jakob Roth
Christian Szepanski

Academic Support and Advisors

Faculty of Aerospace Technology, FH Aachen
Prof. Dr.-Ing. Carsten Braun
Prof. Dr.-Ing. Marc Havermann
Prof. Dr.-Ing. Frank Janser
D. Felix Finger, M.Sc.
Falk Götten, M.Sc.

Submitted on July 1st, 2018

I. Horizon Team



From Left to Right

René Rings

Team Lead

1st semester Aerospace Engineering, Master

Jakob Roth

2nd semester Aerospace Engineering, Master

René Maasmeier

2nd semester Aerospace Engineering, Master

Christian Szepanski

2nd semester Aerospace Engineering, Master

Nils Böhnisch

2nd semester Aerospace Engineering, Master

II. Executive Summary

A team of students from the University of Applied Sciences Aachen has developed an innovative ultra-efficient commercial aircraft concept with an entry into service in 2045. The aircraft allows a reduction of the overall energy consumption by 75% compared to the best in class aircraft from 2005.

In order to reach this result in the conceptual design phase, a reference aircraft was chosen in a first step. After determining the flight mission requirements, the baseline aircraft was resized to calculate a reference energy consumption. Then, a promising aircraft configuration was selected with respect to defined assessment criteria. During the design process, main attention was paid on reducing the total drag, especially the parasitic drag. Besides, it was focused on the integration of a highly efficient propulsion system. In addition to the prementioned aspects, new materials and manufacturing processes were analyzed regarding their structural weight benefits and their estimated technical readiness level in 2045.

In a further step, promising and innovative technologies were investigated with respect to the central design aspects as well as their impact on the energy reduction target set by the NASA N+3 goals. To achieve this aspiring target, it was necessary to build up the conceptual layout with advanced design tools, which are able to consider the integration of trendsetting technologies. The application of this iterative design process led to the conceptual development of Horizon.

Horizon, with its distinctive shape, incorporates a Double Bubble fuselage layout with two ultra-high bypass ratio hybrid-electric driven engines. Furthermore, an Active Aeroelastic Wing with a high aspect ratio shows how the complete Horizon design is driven by cutting edge technology to create a highly efficient aircraft. In addition to the slender wing, a retractable canard for flight states with low velocities is integrated to provide necessary control and trim, as well as auxiliary lift. Parts of wing, fuselage and vertical stabilizer include appropriate technologies to provide laminar flow. Besides these innovative integrations, advanced materials and manufacturing processes are used to reduce the maximum take-off mass of Horizon.

 <p>75% REDUCTION IN ENERGY CONSUMPTION</p>	Total Energy	190.7 GJ
	MTOM	36661 kg
	Design Range	5000 km
	Payload	14250 kg
	Wing Span	34.1 m
	Aspect Ratio	15.46
	Length	33.31 m
	W/S	7525 N/m ²
	P/W	307.3 W/kg
	Fuel Mass	4584 kg
	Battery Mass	2047 kg



III. Contents

- I. Horizon Team I
- II. Executive Summary II
- III. Contents III
- IV. List of Figures IV
- V. List of Tables..... V
- VI. List of Abbreviations and Indices VI

- 1 Introduction 1**
- 2 Approach 2**
- 3 Baseline Aircraft..... 3**
 - 3.1 Mission Requirements and Performance Data 3
 - 3.2 Baseline Resizing 4
- 4 Configuration Selection 5**
 - 4.1 Assessment Criteria 5
 - 4.2 Configuration Analysis and Evaluation 6
 - 4.3 Final Concept Configuration..... 7
- 5 Horizon Concept Technologies 8**
 - 5.1 Structural Layout..... 9
 - 5.1.1 Double Bubble Fuselage 9
 - 5.1.2 Retractable Canard 10
 - 5.1.3 Future Materials 10
 - 5.1.4 Bionic Structures..... 10
 - 5.1.5 Single-Piece Design..... 11
 - 5.1.6 No Cockpit 11
 - 5.1.7 Window-less Fuselage 11
 - 5.1.8 Structural Layout Summary..... 11
 - 5.2 Aerodynamic Design..... 12
 - 5.2.1 Reduction of Wetted Area 12
 - 5.2.2 Lifting Fuselage 13
 - 5.2.3 Laminar Flow Control 13
 - 5.2.4 Boundary Layer Ingestion 14
 - 5.2.5 High Aspect Ratio Wing 15
 - 5.2.6 Flight Mechanical Stability..... 15
 - 5.2.7 Aerodynamic Design Summary 16
 - 5.3 Propulsion System Design 17
 - 5.3.1 Composite Cycle Engine 17
 - 5.3.2 Fuel 18
 - 5.3.3 Electrical Power System 18
 - 5.3.4 Propulsion System Design Summary 19
 - 5.4 Sizing Assumptions 20
- 6 Further Design Aspects 21**
- 7 Horizon Concept Sizing 22**
- 8 Conclusion 25**

- VII. Appendix..... VII
- VIII. References..... VIII

IV. List of Figures

Figure 1 – Design Space of Parallel Hybrid Aircraft.....	2
Figure 2 – A320 Baseline Aircraft.....	3
Figure 3 – A320 Point Performance Results	4
Figure 4 – Final Concept Configuration.....	7
Figure 5 – Technology Overview.....	8
Figure 6 – Horizon Cross Section	9
Figure 7 – Horizon Seat Layout	9
Figure 8 – Bionic Concept Aircraft [38].....	10
Figure 9 – Energy Improvements through Structural Technologies	12
Figure 10 – Lift Distribution Comparison	13
Figure 11 – Wake Filling Principle [22]	14
Figure 12 – Canard Lift over α [25].....	15
Figure 13 – Energy Improvements through Aerodynamic Technologies	16
Figure 14 – Schematic Sketch of the Power Plant.....	17
Figure 15 – Composite Cycle Engine [43]	17
Figure 16 – Flow Path Between Intake and Nozzle	18
Figure 17 – Specific Battery Energy Sensitivity	19
Figure 18 – Energy Improvements through Propulsion Technologies	20
Figure 19 – Assumed Technological Improvement.....	20
Figure 20 – Horizon Matching Diagram.....	22
Figure 21 – Horizon Three-View	25

V. List of Tables

Table 1 – NASA Subsonic Transport System Level Metrics	1
Table 2 – A320 Requirements and Performance.....	3
Table 3 – A320 Flight Mission and Energy Distribution	4
Table 4 – A320 Mass Breakdown	5
Table 5 – Analyzed Configurations	6
Table 6 – Comparison of Different Aircraft Configurations	7
Table 7 – Horizon’s Key Technologies	8
Table 8 – Structural Technologies.....	11
Table 9 – Comparison Wetted Area	12
Table 10 – Aerodynamic Technologies	16
Table 11 – Battery Systems [48, 49, 44, 50, 51].....	18
Table 12 – Propulsion Technologies	19
Table 13 – Horizon Flight Mission and Energy Distribution.....	23
Table 14 – Horizon Requirements and Performance	24
Table 15 – Horizon Mass Breakdown.....	24

VI. List of Abbreviations and Indices

Abbreviation	Description
AAW	Active Aeroelastic Wing
A/P	Autopilot
AR	Aspect Ratio
ASCS	Active Stability Control System
BLI	Boundary Layer Ingestion
BSFC	Break Specific Fuel Consumption
UBPR	Ultra-High Bypass Ratio
CCE	Composite Cycle Engine
CMC	Ceramic Matrix Composites
CNT	Carbon Nanotubes Still
DFCS	Digital Flight Control System
EIS	Entry into Service
EM	Electric Motor
GTF	Geared Turbofan
H _E	Degree of Hybridization of Energy
H _P	Degree of Hybridization of Power
ICE	Internal Combustion Engine
J	Joule (Unit of Energy)
LD	Landing
LFC	Laminar Flow Control
MZFM	Maximum Zero Fuel Mass
P/W	Power-to-Weight Ratio
PAX	Passengers
PreHyST	Preliminary Hybrid Sizing Tool
RoC	Rate of Climb
T/W	Thrust-to-Weight Ratio
TO	Take-off
TLAR	Top-Level Aircraft Requirements
TRL	Technology Readiness Level
TSFC	Thrust Specific Fuel Consumption
nc	Non-Consumable

1 Introduction

With steadily increasing world population and urbanization, the growth of global air traffic is accelerating incessantly. In contrast, the environmental effects of aircraft and the limited resources of fossil fuel call for a reduction in energy utilization for aviation. NASA, as well as the European Commission, imposed ambitious targets for air transport concerning the environmental protection, referred to as the N+ goals (see Table 1) and the Flightpath 2050. In order to fulfill these targets, it is necessary that new aircraft concepts are developed, which are much more efficient than currently existing aircraft. While on the one hand, these concepts must comprise advanced technologies and consider configurational changes to achieve the aspiring goals, on the other hand, they have to withstand the demanding requirements of aviation in regard to safety and reliability.

This project aims to combine both tasks by developing an ultra-efficient commercial aircraft, named Horizon, which has an entry into service (EIS) in 2045. In relation to the N+3 goals, Horizon is primarily designed to improve the energy consumption in flight by at least 60% in comparison to the best in class aircraft of the year 2005, whereas the long-term objective is a reduction of 80%. Additionally, the reduction of emissions and noise are central design aspects considered in the conceptual design of this innovative aircraft.

In the following sections, the development of Horizon is presented, while, in a first step, the baseline flight mission and the reference energy are determined by resizing the best in class aircraft of 2005. Based on defined criteria, multiple aircraft configurations are discussed to ensure a systematic and objective selection process that leads to the final choice of the Horizon configuration. Thereafter, Horizon's key technologies are described, which are selected with respect to parameters like drag (especially wetted area [1]), weight and propulsive efficiency. Their particular capabilities of decreasing the energy consumption of the concept plane are described in detail. This includes technologies that improve the structural layout, the aerodynamic design and especially the propulsion system design, where a parallel hybrid-electric propulsion system offers new degrees of freedom for the overall design of Horizon. Furthermore, operational aspects, passenger acceptance and the certification are considered. In a final step, the preliminary sizing of the Horizon concept is shown, which specifies the dimensions and the masses of the novel aircraft. Therefore, it enables the comparison of total energy and reference energy to evaluate the ability of the aircraft to meet the goal of an 80% improvement in energy consumption.

Table 1 – NASA Subsonic Transport System Level Metrics

Technology Benefits	Technology Generations (Technology Readiness Level 5-6)		
	short term (N+1) 2015-2025	medium-term (N+2) 2025-2035	long-term (N+3) after 2035
Noise (cum margin rel. to Stage 4)	22-32 dB	32-42 dB	42-52 dB
LTO NOx Emissions (rel. to CAEP 6)	70-75 %	80 %	> 80 %
Cruise NOx Emissions (rel. to 2005 best in class)	65-70 %	80 %	> 80 %
Fuel/Energy Consumption (rel. to 2005 best in class)	40-50 %	50-60 %	60-80 %

2 Approach

In order to resize the reference aircraft and to perform a complete preliminary sizing of Horizon, a new sizing algorithm is used, which is able to deal with several kinds of propulsion configurations, including conventional powered aircraft and parallel hybrid powered aircraft.

One of the outstanding characteristics of this algorithm is the capability to identify the optimum design point and the optimal degree of hybridization (H_P) (see Equation 1) of electrified aircraft in regard to defined design objectives (e.g. MTOM, energy). For that purpose, the algorithm divides the overall power demand arising from the top-level aircraft requirements (TLAR) to the electric motors (EM) and the internal combustion engines (ICE) for a large number of design points (see Figure 1). For each design point, MTOM and total energy are calculated and the optimum design point is searched for.

$$H_P = \frac{P_{EM,max}}{P_{max}} \quad (1)$$

Another specialty of the algorithm is the innovative way in which the energy carrier masses (e.g. fuel, batteries) are calculated, as the transport energy which is needed in small time steps of each mission segment, is analyzed. The application of this procedure is a result of the impracticality of statistical fuel fractions for electrified aircraft.

The methodology of this algorithm involves classical preliminary aircraft analysis methods as presented by Raymer [2] or Gudmundsson [3], while the algorithm is implemented into the software tool *PreHyST*. A detailed description of the tool can be found in Rings [4] and Ludowicy [5].

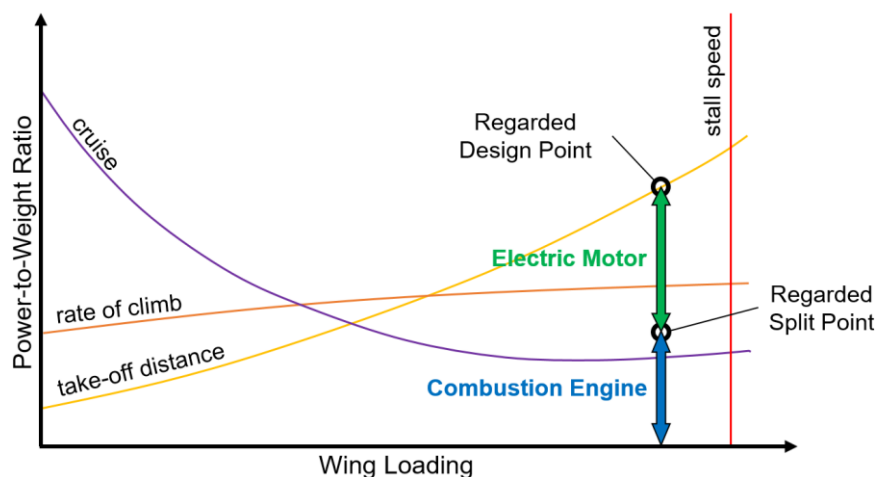


Figure 1 – Design Space of Parallel Hybrid Aircraft

PreHyST provides accurate calculations of the energy consumption in flight and initial estimations of the MTOM, the required thrust or power as well as the wing area. The tool requires aerodynamic data and information about structural masses as inputs. Therefore, several handbook methods are used to deliver this data. Structural masses for the baseline aircraft are calculated by means of semi-empirical equation methods by Kundu [6] and are compared to a statistical method offered by Raymer [2]. As the dimensions of the Horizon aircraft are unknown before the initial sizing, the structural masses of the baseline aircraft are used as a starting point. These are merged with the mass improvement assumptions made in chapter 5.1. Aerodynamic data, especially in terms of parasitic drag, is primarily generated using methods given in the USAF DATCOM [7] within the scope of analyses with NASA's open source tool *OpenVSP*.

3 Baseline Aircraft

The central objective of the Horizon concept is to reduce the total energy consumption in flight by 80% relative to the best in class aircraft of the year 2005 (see Table 1). This leads to the specification of a baseline aircraft and the determination of a reference energy being an indispensable and elementary step during the design process of the ultra-efficient aircraft. Simultaneously, the baseline aircraft defines the flight mission for the new airplane and sets the requirements, which must be fulfilled. Within the scope of this concept study, the comparison baseline is the Airbus A320-200, equipped with two CFM56-5A3 turbofan engines, as depicted in Figure 2.



Figure 2 – A320 Baseline Aircraft

In the following sections, mission requirements and performance data of the A320 are presented and results of the resizing are illustrated.

3.1 Mission Requirements and Performance Data

The mission requirements define the dimensions and the performance of a new aircraft and thus are highly significant parameters in aircraft design. In its design point (see Figure 3), the A320 is able to carry a payload of 14250 kg (150 PAX) over a design range of 5000 km [8], as defined by the payload-range diagram [9]. In cruise, the Airbus operates at flight level 370 with a Mach number of 0.78, while the maximum achievable altitude is reached at 12130 m [10]. The reference aircraft is designed to accomplish a maximum rate of climb (RoC) of 12.2 m/s shortly after take-off. The minimum take-off distance at mean sea level conditions for the A320 is given with 2180 m and the landing distance is specified with 1440 m [8]. The presented TLARs are summarized in Table 2 and are used for the initial sizing of the baseline (see chapter 3.2).

Further requirements for the initial sizing are the aerodynamic performances at take-off and landing, as well as the stall behavior and the performance of the propulsion system. During take-off, the baseline aircraft achieves a flapped maximum lift coefficient of 2.56, whereas the corresponding coefficient for landing is 3.0 [8]. According to Roskam [11], the maximum lift coefficient in clean configuration is estimated to be 1.5. Using NASA's *OpenVSP*, a minimum parasitic drag coefficient ($C_{D,min}$) of 0.0235 is determined for cruise flight. In combination with lift-dependent drag, the maximum lift-to-drag ratio (L/D) is calculated to be 19.7 by means of the basic lift- and drag polar formulas [3]. Concerning the performance of the propulsion system it is assumed that the turbofan engines of the reference aircraft operate at a TSFC of 0.543 kg/kg/h in cruise [12]. In Table 3, the flight mission of the Airbus A320 is illustrated, which also corresponds to the mission profile for Horizon.

Table 2 – A320 Requirements and Performance

Parameter	Unit	Value
TLARs		
Payload	kg	14250
Range	km	5000
Cruise Velocity	m/s	230
Cruise Altitude	m	11280
Service Ceiling	m	12130
Rate of Climb	m/s	12.2
Take-off Distance	m	2180
Landing Distance	m	1440
Aerodynamics		
$C_{L,max}$	-	1.50
$C_{L,max,TO}$	-	2.56
$C_{L,max,LD}$	-	3.00
$C_{D,min}$	-	0.0235
L/D_{max}	-	19.7
L/D_{cruise}	-	18.8
Propulsion System		
$TSFC_{min}$	kg/kg/h	0.454
$TSFC_{cruise}$	kg/kg/h	0.543

3.2 Baseline Resizing

Once all requirements and performance data are known, the baseline aircraft is resized and the reference energy can be determined. In a first step, a so-called constraint analysis is performed as introduced by Loftin [13] and extended by Gudmundsson [3]. Therefore, using the *PreHyST* software tool, the optimum design point of the A320, in regard to the recently defined requirements, is identified in the matching diagram (see Figure 3), considering the design rule for conventional powered aircraft [14, 3]. The constraint analysis provides an optimum thrust-to-weight ratio (T/W) of 0.327 at a wing loading (W/S) of 5891 N/m².

In a second step, the MTOM and accordingly the required fuel mass is calculated in the mission analysis. This requires knowledge about the design point and the empty mass fraction in order to simulate the flight mission presented in Table 3. The empty mass fraction results from the calculation of the structural masses using Kundu's class II equations. The masses are included in the overview of the mass breakdown for the A320 (see Table 4). Within the scope of this mission analysis, also the mass of the propulsion system is specified. The dry engine masses and the masses of the engine mounts are computed with respect to the maximum required thrust, in accordance to methods offered by Raymer [2].

The reference energy is a result of the mission simulation, since it is associated with the fuel mass by its calorific value. Thus, the reference energy, in contrast to the transport energy, incorporates the whole propulsive efficiency, which offers an improved comparability of the energy needed by Horizon. This is advantageous, as the concept plane includes a parallel hybrid propulsion system, which entails an efficiency chain with much more components. Taking all assumptions into account, a total mission energy of 758.9 GJ is determined for the reference mission flown by the 2005 state of the art A320. The distribution of the energy in the respective flight segments is showcased in the table below. It has to be noted that the energy for acceleration phases is not specified.

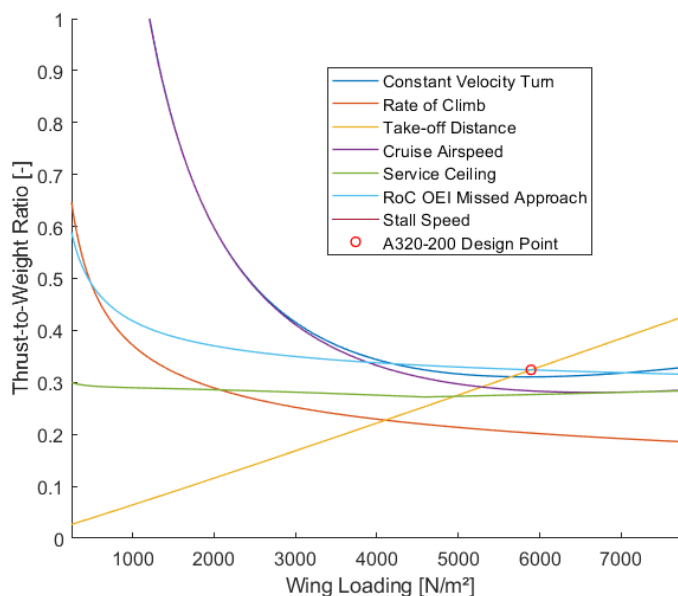


Figure 3 – A320 Point Performance Results

Table 3 – A320 Flight Mission and Energy Distribution

Mission Segment	Taxi-in	Take-off	Climb	Cruise	Descent	Loiter	Descent	Landing & Taxi-out
Time [min]	15	0.55	-	-	-	60	-	15
Distance [km]	-	-	261	5000	162	-	60	-
Airspeed [m/s]	9.5	67	115 to 213	230 (Ma 0.78)	194 to 120	130	117 to 100	9.5
Energy [GJ]	28.97	3.80	67.79	485.79	16.33	104.58	15.62	28.93

With the mission analysis being completed, the particular masses of the reference aircraft are known. MTOM, fuel mass and mass of the propulsion system are the central outputs of the described sizing tool. The payload mass is a function of the number of passengers and thus, is a central requirement. The structural masses, as well as the masses of systems and equipment, are given by Kundu’s equations in dependence on the MTOM, taking into account important aircraft geometry parameters. However, as mentioned above, the MTOM is a result of the mission performance sizing. Accordingly, it can be multiplied to obtain the total values of the masses for structure, systems and equipment.

$$MTOM = \left(\frac{m_{empty}}{MTOM}\right) \cdot MTOM + m_{fuel} + m_{payload} \tag{2}$$

In Table 4, a mass breakdown of the resized Airbus A320 is given, including the specified categories and components. Additionally, the maximum zero fuel mass (MZFM) for the design point of 5000 km range and 14250 kg payload is highlighted.

Table 4 – A320 Mass Breakdown

Group	Mass [kg]	% MTOM	Group	Mass [kg]	% MTOM
Structures	23494	31.82	Systems and Equipment	8296	11.23
Wing	8752	11.85	Miscellaneous	4393	5.95
Horizontal Tail	1914	2.59			
Vertical Tail	550	0.74			
Fuselage	7732	10.47			
Landing Gear	2965	4.02			
Nacelles	1581	2.14	Operating Empty Mass	40840	55.31
Propulsion	4657	6.31	Useful Load	33004	44.69
Engines	4562	6.18	Payload	14250	19.30
Engine Mounts	95	0.13	Fuel	18754	25.40
			Maximum Zero Fuel Mass	55090	74.60
			Maximum Take-off Mass	73844	100.00

4 Configuration Selection

An essential part within the conceptual design phase is the comparison and evaluation of different configurations regarding their advantages and disadvantages. In this chapter, several aircraft configurations are assessed using rating criterions. As a result of this process, the general configuration of Horizon is chosen.

4.1 Assessment Criterions

At first, the main triggers of an innovative aircraft are specified. Regarding the N+3 goals (see Table 1), the following aspects have the most promising impact on the configuration selection:

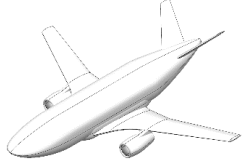
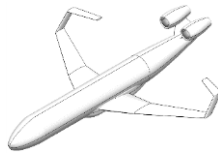
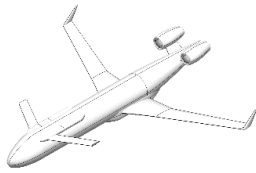
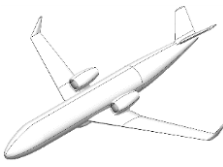
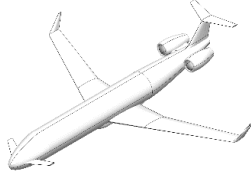
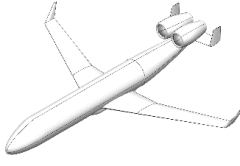
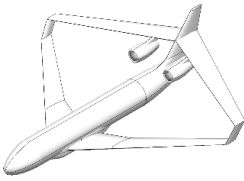
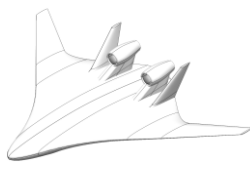
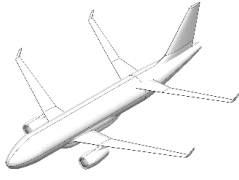
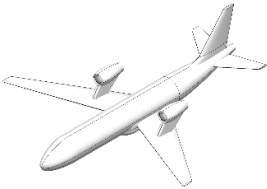
- Reduction of viscous drag
- Reduction of structural mass
- Highly efficient propulsion

Furthermore, improvements in terms of manufacturing processes and advanced materials drive a configuration’s layout regarding weight savings, respectively.

4.2 Configuration Analysis and Evaluation

Starting with different configurations, the varying characteristics are analyzed. Main differences include the wing design, the possible engine position, the empennage arrangement and the fuselage layout.

Table 5 – Analyzed Configurations

	<ul style="list-style-type: none"> + Provides space for BLI & Canard + Shorter fuselage - Slightly increased wetted area 		<ul style="list-style-type: none"> + Reduction in induced drag - Intersections lead to interference drag - Control difficulties
Double Bubble		C-Wing	
	<ul style="list-style-type: none"> + Decreased wetted area + Decreased interference drag + Stability - Complex mechanics 		<ul style="list-style-type: none"> + Shorter landing gear → mass + Reduction of viscous drag & interference - Complex controlling & trimming
Tailless Canard		V-Tail (Overwing Engines)	
	<ul style="list-style-type: none"> + Stability - Increased interference drag 		<ul style="list-style-type: none"> + Noise shielding - Maintenance of engines
Three Surface		U-Tail	
	<ul style="list-style-type: none"> + Reduction of induced drag - Increase of interference drag - Complex geometry - Operations 		<ul style="list-style-type: none"> + Reduction of interference drag + Carry over lift - no windows → acceptance - Operations - Manufacturing
Box Wing		Blended Wing Body	
	<ul style="list-style-type: none"> + Reduction of induced drag - Increase of interference drag - Operations 		<ul style="list-style-type: none"> + Reduction of cross flow + Noise shielding - Increase of induced drag - Complex geometry - Operations
Tandem Wing		Forward Swept Wing (Overwing Engines)	

In order to achieve the largest possible reduction in energy consumption, the main focus during the evaluation is laid on aerodynamic efficiency, since the greatest potential is expected in this area. Nevertheless, the influence of structural mass and propulsive efficiency is considered as well.

To get an overview of many different characteristics and their impact on total drag, the following evaluation table is set up. For more precise statements, scoring and weighting factors are introduced. The weighting factors are chosen according to their potential for energy savings. Since the viscous drag is easier to influence with different configurations, the highest weighting factor of 0.45 is assigned. While the induced drag represents the second largest influence with a factor of 0.35, the interference drag, as smallest influence, only weighs in with 0.2.

Table 6 – Comparison of Different Aircraft Configurations

Configuration	Interference Drag	Induced Drag	Viscous Drag	Score	Ranking
Blended Wing Body	2	-1	-1	-0.4	10
Tandem Wing	-2	1	-1	-0.5	11
Joined Wing	-3	1	-1	-0.7	12
Box Wing	-2	3	-2	-0.25	9
Forward Swept Wing	0	-1	0	-0.35	7
Strutted Wing	-2	1	0	-0.05	5
C-Wing	-1	2	1	0.95	2
Three Surface	-2	1	0	-0.05	5
Tailless Canard	1	1	2	1.45	1
V-Tail	1	0	1	0.65	3
U-Tail	0	0	0	0	4
Double Bubble	1	0	-1	-0.25	7
Weighting Factor	0.2	0.35	0.45	1	

The chosen configurations are rated with values between -3 and +3 in the different drag categories. While ratings of -3 are not favorable, +3 ratings promise a high reduction in total drag. As a final result, each configuration is weighed and summed up in one score.

Aircraft layouts with many intersecting components, like the Joined Wing, the Tandem Wing and the Box Wing (see Table 5) lead to a high amount of interference drag and thus, negative evaluation values. Better interference behavior is reached by the Blended Wing Body, the Tailless Canard and the Double Bubble configuration. Having a look at the induced drag, three parameters have to be taken into account: lift coefficient, aspect ratio and Oswald factor. Configurations with low AR, like the Blended Wing Body, are rated with negative values. In contrast, aircraft with well-shaped wingtips and favorable lift distributions, like the C-Wing or the Box Wing, are rated with high positive values (see Table 6). Configurations with increased wetted area, like the Blended Wing Body, are provided with negative evaluation values for the viscous drag rating. In contrast to that, configurations with a reduced surface, like the Tailless Canard or the V-Tail, are rated with positive values.

As shown in Table 6, the highest score is achieved by the Tailless Canard configuration with a score of 1.45. Additionally, the C-Wing and the V-Tail configuration (see Table 5) achieve positive scores with values of 0.95 and 0.65, respectively.

4.3 Final Concept Configuration

Based on the previous drag considerations, the final concept configuration is chosen to be a tailless canard arrangement (see Table 5). To find the optimal layout, the selection and integration of the propulsion system must be taken into account, as mentioned in chapter 4.1. Thus, positioning the engines in the rear section of the aircraft allows for unconventional propulsion configurations, as described in a later section (see chapter 5.3). These can be beneficial as it allows to include boundary layer ingestion (BLI) engines and counters possible batteries at the front. A high aspect ratio (AR), low-wing design is introduced into the design to minimize induced drag. With the lift-generating canard, improvements in aerodynamics and controllability are expected.

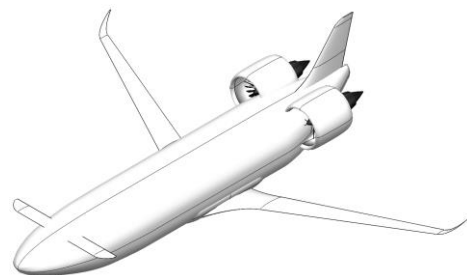


Figure 4 – Final Concept Configuration

Differing from the pure Tailless Canard configuration, a combination with the Double Bubble fuselage configuration is selected. This aims at unique advantages in terms of additional lift and trim drag (see chapter 5.1.1, 5.2.2). To improve the Tailless Canard configuration towards a more feasible aircraft concept with respect to lateral stability, a vertical stabilizer is integrated. As a consequence, an increase in overall wetted area has to be accepted. Further advantages due to the application of innovative technologies are described in the following chapters.

5 Horizon Concept Technologies

The Horizon concept design applies several future technologies within all major engineering fields to achieve the mentioned goal in total energy savings (see chapter 1). In the following sections, the most promising technologies will be discussed in detail and are directly related to drag and weight reductions as well as feasibility aspects, like the technology readiness level (TRL). The technology applications are divided into structural layout (see chapter 5.1), aerodynamic design (see chapter 5.2) and propulsion system Design (see chapter 5.3).

Note: All mentioned savings in total energy consumption are based on single-technology-sizing with respect to the A320 baseline aircraft (see chapter 3). The single improvements stated are not to be mistaken with the final sizing calculation, which merges all technologies in concluding mass and drag considerations. These estimations for the combination of all applied technologies are presented in chapter 7.

Table 7 – Horizon’s Key Technologies

Technology	Chapter	Reference
Double Bubble Fuselage	5.1.1, 5.2.2	[15, 16, 17]
Active Aeroelastic Wing	5.2.5	[18, 19, 20, 21]
High Bypass Composite Engines with Boundary Layer Ingestion	5.2.4, 5.3.1	[22, 23, 24]
Retractable Canard	5.1.2, 5.2.6	[25, 26]
Active Laminar Flow Control	5.2.3	[27, 28, 29, 30, 31]
Bionic Structures	5.1.4	[32]
Future Materials	5.1.3	[33, 34, 35, 36]
Single-Piece Design	5.1.5	[37]

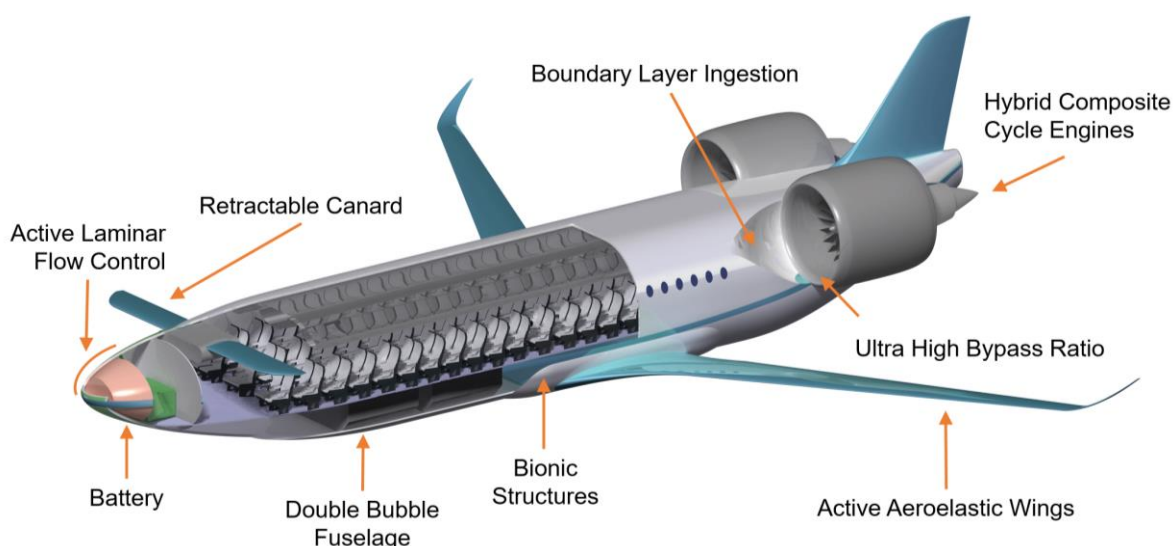


Figure 5 – Technology Overview

5.1 Structural Layout

In the following section, all applied structural features will be evaluated in detail, laying the focus on the mass savings throughout the entire aircraft structure.

5.1.1 Double Bubble Fuselage

The Horizon concept applies a wide fuselage configuration, aiming at the beneficial aerodynamic features that emerge with this so called “Double Bubble” fuselage (see chapter 5.2.2) [16].

To achieve a nearly unchanged level of wetted area for the fuselage compared to the A320 fuselage, a tradeoff study was carried out, resulting in the new geometric proportions shown in Figure 6. The width of the concept fuselage increased by about 34% compared to the baseline aircraft, allowing for a higher number of seats per row. The length in this geometric tradeoff could be reduced correspondingly by 17.5%. The resulting Horizon cabin layout consists of a two-class, two-aisle, 2-4-2 seat configuration with cabin dimensions as seen in Figure 6.

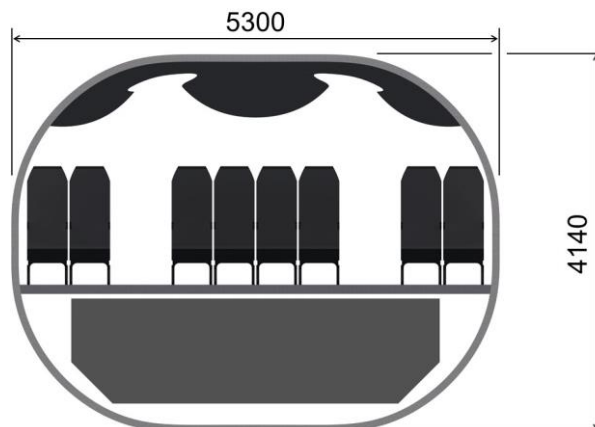


Figure 6 – Horizon Cross Section

For the business class, a 2-2-2 layout is included to allow the fuselage to narrow down gradually towards the nose as well as to enhance passenger comfort. While the engines safety zone does not permit a rear entrance into the cabin, the two-aisle design (see Figure 7) complies certification specifications with respect to emergency evacuation over one front exit and two over wing exits on each side.

From a structural point of view, this configuration comes with one major challenging aspect that needs to be addressed: Due to cabin pressurization of the non-circular fuselage cross section, the wall structure has to cope with increased circumferential stresses and fatigue. The Horizon concept compensates for this issue by reinforcing the fuselage skin at critical angular positions. A solution with positioning intermediate struts throughout the cabin as vertical support did not seem up to date in the 2045 timeframe.

While the circumferential loads are increased, the shortened fuselage length reduces longitudinal loads and bending moments inside the fuselage structure, thus allowing for a lighter construction. Assessing the tail assembly regarding loads, the missing horizontal stabilizer relieves the rear structure in the vertical direction by reducing its weight and aerodynamic loads. However, the rear-mounted high bypass ratio engines counteract this improvement. The engines mass, the thrust and aerodynamic loads on the nacelle require a reinforced rear structure.

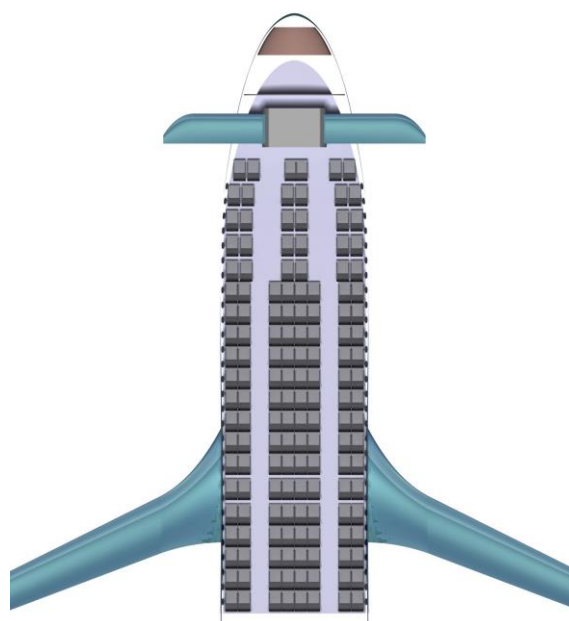


Figure 7 – Horizon Seat Layout

5.1.2 Retractable Canard

The Horizon concept is designed to deploy a front-mounted retractable canard system, when operating in take-off, climb, descent and landing (see chapter 5.2.6). The implementation of such an advanced system is another challenge to overcome but is a proven technology [25]. A good example for the integration of a similar canard system can be found on the Tupolev TU-144 [26]. When considering the layout and volume management of the aircraft's front section, the canard system is best placed between the battery compartment in the nose and the first cabin door.

5.1.3 Future Materials

One promising way towards a significant mass reduction are future materials. Lowering structural mass, while maintaining the ability to cope with the emerging loads on the aircraft is a key for achieving the mentioned goal (see chapter 1).

The application of future materials will allow many components of the aircraft structure to be lighter while maintaining their required structural strength and stiffness. Despite the research in carbon nanotubes (CNT) still being at the beginning, a game-changing increase in quality and quantity is expected. Especially the use of CNT in fiber composites is promising a huge increase in strength-to-weight-ratio. With values reaching up to 60000 kNm/kg, CNT theoretically surpasses state of the art carbon fiber by 20 times in specific strength [33]. Besides CNT, other possibly game-changing materials are graphene and colossal carbon tubes, variations of the single carbon atom layer category [34].

For structural CNT applications a weight reduction of 30% is estimated in the near future, demonstrating the potential of this future material [35]. Regarding feasibility of CNT applications, the TRL is expected to increase rapidly due to the high demand and competition, reaching operations status in the 2045 timeframe [36].

The application of future materials leads to an estimated improvement in total energy consumption of 27.6% with respect to the baseline aircraft.

5.1.4 Bionic Structures

A bionically optimized structural shape distributes the acting loads more gradually throughout the aircraft's structure. This procedure ensures a mass reduction of many oversized components and reinforcements. During the optimization, the specific part undergoes an iterative process wherein the part-design and stress analysis adapt the structure in between set interface boundaries to evenly distribute the stress [32].

Using future 4D printing technologies will allow the aircraft structure to incorporate an additional information regarding the shapes of certain components. This fourth component can be controlled via electrical signals to automatically adapt the shape to the desired flight condition. Another possible control mechanism could be an independent intelligent behavior which uses the ambient atmospheric conditions like pressure or temperature as control input for the morphing bionic structure. For the application of the innovative printed bionic structures, an improvement of 24.3% is expected.



Figure 8 – Bionic Concept Aircraft [38]

5.1.5 Single-Piece Design

Reducing the total number of components in overall assemblies and working towards more one-piece designs will reduce weight by getting rid of mechanical fasteners and adhesive joints. This also improves the structural integrity of these components. Additionally, the one-piece design leads to a more direct manufacturing process, reduced accessibility problems during assembly as well as less maintenance tasks. Applications in full barrel fuselage and nacelle designs have successfully been tested [37].

For this technological application, an improvement in energy consumption of 17.4% is achieved.

5.1.6 No Cockpit

Over the last couple of decades, the number of acting pilots and board engineers has decreased constantly, while autopilot systems have taken over large portions of the flight mission. With autonomous systems improving rapidly, the Horizon concept uses pilotless flying, seeing its feasibility after the next three decades. By removing the cockpit structure, instruments and avionics, mass and build-volume in the aircraft front section is saved.

5.1.7 Window-less Fuselage

Another chance to reduce the mass and thus the energy consumption of the aircraft is a window-less fuselage configuration. Future lightweight screen applications or future VR technologies can cover the cabin walls as window replacement. Mass estimations for the baseline A320 windows show a reduction of about 390 kg, resulting in 1% total energy savings. Yet, for the sake of passenger acceptance and comfort, the Horizon concept does not apply this technology. The real view out of an aircraft window is still hard to beat.

5.1.8 Structural Layout Summary

The following structural technologies are incorporated by the Horizon concept plane:

- Future Materials
- Printed bionic structures
- Single-piece design

In Table 8 the overall improvements in operating empty mass are presented, while only applying the structural technologies. It must be noted that all values are given as potential improvements regarding the baseline aircraft. In Figure 9, an overview over the energy improvements achieved by the individual technologies is delivered.

Table 8 – Structural Technologies

Technology	Parameters	Improvement [%]
Future Materials	OEM ¹	15
Printed bionic structures	OEM	12.7
Single-piece design	OEM	8.3
Window-less	OEM	0.43

¹ without propulsion system mass

The consideration of the window-less fuselage solely serves for demonstrational means. It is not a technology used for the Horizon aircraft, as specified in 5.1.7.

see important Note on Page 8

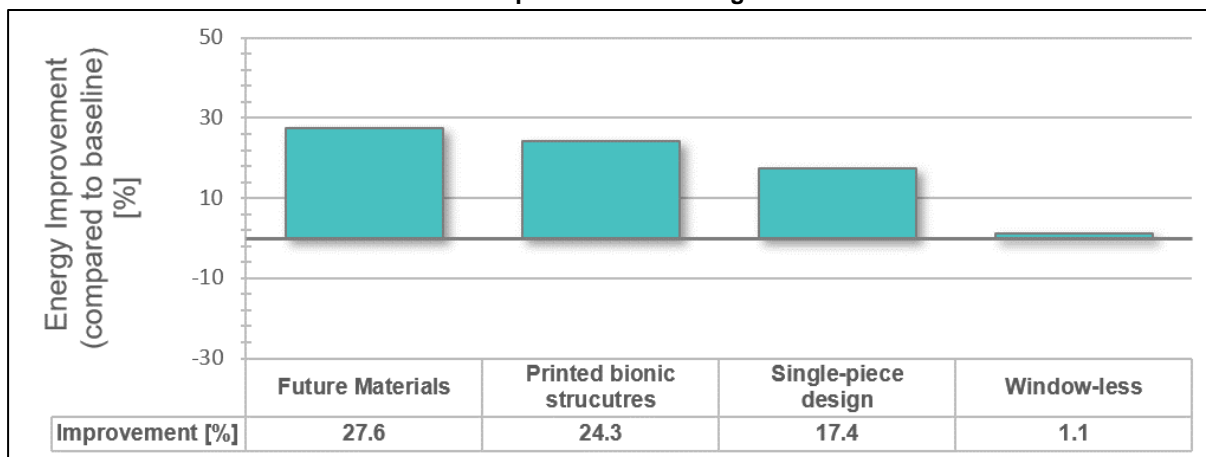


Figure 9 – Energy Improvements through Structural Technologies

5.2 Aerodynamic Design

In order to reduce the overall drag and to achieve the N+3 goals, Horizon is provided with several aerodynamically advanced technologies. Horizon also aims towards a reduction of wetted area by including a drag optimized configuration. In the following section the particular measures are described.

5.2.1 Reduction of Wetted Area

The largest drag contributors are the viscous drag and the lift induced drag, together producing approximately 80% [39] of the overall drag. They occur due to skin friction and vortex formation at the wing tips, respectively. Hence, there is a large potential for drag reduction. Due to the change of the overall configuration the reduction of the wetted surface area decreases the viscous drag significantly.

The surface wetted area breakdown of Horizon’s components and a comparison with the A320 can be seen in Table 9. It is shown that the overall wetted area is reduced by approximately 23%. The largest improvements are generated by the canard (cf. A320’s horizontal stabilizer). Because of the retractability during cruise the wetted area of the canard can be reduced to zero and leads to a further reduction of the viscous drag.

Table 9 – Comparison Wetted Area

Component	A320 S_{wet} [m ²]	Horizon S_{wet} [m ²]	Improvement [%]
Fuselage	362.23	375.19	-3.58
Main Wing	203.89	98.13	51.87
Engines	52.3	51.06	2.37
Vertical Stabilizer	49.02	21.74	55.65
Horizontal Stabilizer	47.69	14.09	70.46
Belly Fairing	47.61	39.47	17.10
Pylon	13.45	0	100
Winglets	1.9	0 ¹	100
Summation	778.09	599.68	22.93

¹ considered in the main wing

Since the engines are integrated into the rear part of the fuselage, the pylon’s wetted area is also completely erased. The Active Aeroelastic Wing (AAW) as well as the vertical stabilizer both have a reduced wetted area compared to the A320. This results from the expected reduction in weight since the required lift, which is mainly influenced by the wing area, is decreased.

In contrast to these improvements stands the Double Bubble fuselage, where the wetted area is approximately 3% enlarged. This is due to the fact that it is impossible to scale down the fuselage, because the volume for passengers and cargo has to remain constant [1].

Moreover, other factors have to be considered for the comparison of the wetted area. On the one hand, the intersection with other components plays a role. More intersections reduce the wetted area of the assembled component and increase interference drag. Because Horizon's fuselage has less intersections, the related wetted area becomes larger.

In summary the wetted area is reduced by approximately 23% compared to the baseline aircraft. This leads to an energy efficiency improvement of approximately 30%, as depicted in Figure 13.

5.2.2 Lifting Fuselage

During the fuselage design, the fuselage proportions are analyzed with respect to aerodynamic benefits. Even though the wetted area of the Double Bubble fuselage is increased (see Table 9), advantages according to aerodynamic efficiency and trimmed stability are recognized.

One benefit compared to conventional fuselage layouts is the increase of fuselage-carried lift due to the extended fuselage width (see Figure 10) [16].

As an effect of a fuller lift distribution, the wing can be scaled down, which further reduces the wetted area [16]. Besides, the bell-shaped lift distribution maximizes aerodynamic efficiency and enables the reduction of the vertical tail size due to beneficial roll-yaw coupling [17]. Furthermore, the Double Bubble fuselage layout achieves a more favorable nose-pitching moment due to the raised front section [15]. Additionally, a shorter cabin reduces the possible position of the center of gravity [16].

Next to the aerodynamic effects, the wide fuselage layout is beneficial for the integration of the retractable canards and the BLI turbofan engines. Further structural characteristics of the Double Bubble are described in chapter 5.1.1.

Based on these aerodynamic as well as structural advantages, the Double Bubble fuselage is chosen for the Horizon concept.

5.2.3 Laminar Flow Control

One of the most promising technologies in drag reduction is the achievement of laminar flow. Since the viscous drag depends strongly on the flow characteristic (laminar or turbulent), the goal is to obtain a laminar flow over the aircraft's surfaces.

Research shows that a reduction of 60% in overall viscous drag can be obtained by using Laminar Flow Control (LFC) on the wing, stabilizer and fuselage [27]. This is achieved via boundary layer suction of the aircraft's surfaces with pumps and porose skins [27]. A total reduction in viscous drag of 56% can be reached for wing and tail, and 65% for the fuselage [27]. Differing from the expected improvements described by Beck et al. [27], the assumptions for Horizon's improvements of the viscous drag are limited to 40% for the wing and 50% for the vertical stabilizer. These conservative

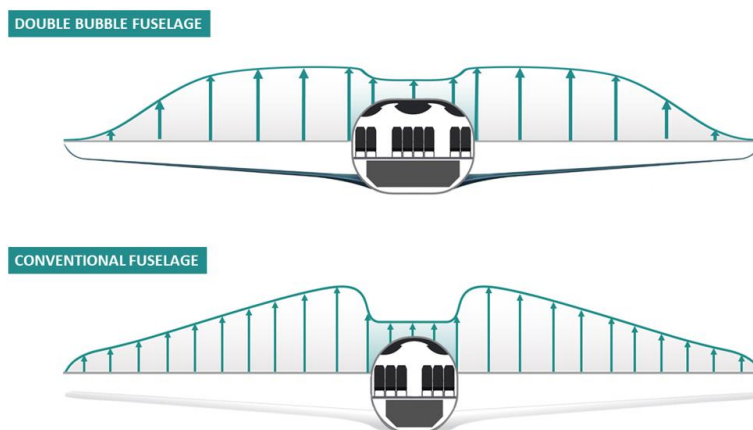


Figure 10 – Lift Distribution Comparison

assumptions are considerations with respect to the complex integration in the AAW with morphing flaps and slats, as well as with respect to transonic effects occurring during flight. This also ensures a conservative contemplation.

Because the concept is furtherly designed with engines enabling BLI, LFC is only applied in the front part of the fuselage. Thus, the viscous drag reduction of the fuselage is limited to approximately 20%.

One drawback of this technical realization is the additional mass due to the systems. The LFC system weight penalty (e.g. suction pumps, pipes) is computed to be approximately 9% of the fuselage mass, as well as 18% of the main wing's and the vertical stabilizer's mass. These values are in accordance with the assumptions made by Beck et al. [27].

With respect to the innovative production methods described before (see chapter 5.1), new possibilities of LFC system integration arise. The pumps can be located in the bottom part of the fuselage while the necessary plenums are integrated in the fuselage skin.

Flow instabilities, like attachment line and cross flow instabilities can influence the boundary layer. To avoid cross flow instabilities another technology could be used in the Horizon concept. With plasma actuators the transition point from laminar to turbulent boundary layer flow can be delayed [28]. Current research shows that it is possible to control the flow via plasma actuators [29, 30]. Due to the relatively low TRL and some unsolved problems like enhancing the turbulence at certain frequencies [31], this system is only an option with respect to the avoidance of flow instabilities and preclude turbulent flow.

In summary, Horizon is provided with a suction technology and laminar flow is maintained almost half over the wing and the vertical stabilizer. In addition, the front part of the fuselage is maintained laminar, further decreasing the viscous drag. The overall structural mass is increased by 6.5%. A total energy improvement of approximately 15% can be reached by using LFC.

5.2.4 Boundary Layer Ingestion

As mentioned, the fuselage-integrated engines are also used for BLI. Due to the fact that the engines are integrated into the fuselage, the mass flow sucked by them can be used to ingest the low velocity boundary layer [23]. By ingesting an amount of the boundary layer, the viscous drag is reduced by a wake filling which leads to a more uniform velocity profile (see Figure 11) [22].

The best possible propulsion concept is a "cylindrical fuselage with circumferential fan at the aft section (PROPFUS)" [22], where the viscous drag of the fuselage can be reduced by 80% [22]. Horizon has two engines, which do not have a circumferential fan like the PROPFUS. Thus, it is comparable to the REVOLVE concept, which includes "aft-mounted fans covering the upper part of a cylindrical fuselage" [22], where one-third of the fuselage is covered with fans. This results in a viscous drag reduction of 26% for the fuselage. A further analysis presents an energy efficiency improvement of approximately 8% for BLI, as installed in the developed aircraft.

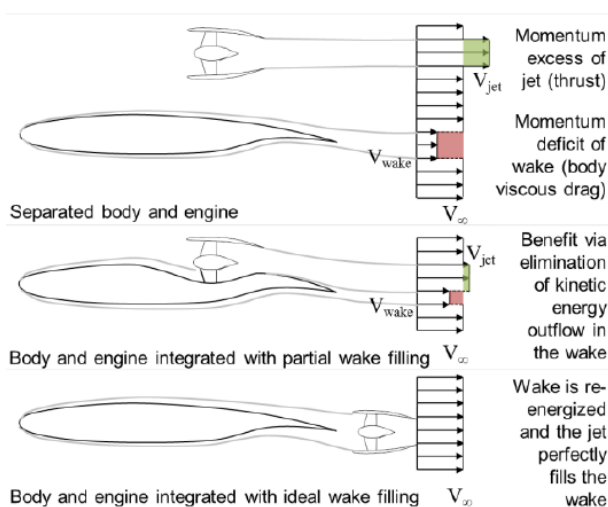


Figure 11 – Wake Filling Principle [22]

5.2.5 High Aspect Ratio Wing

The main difference in Horizon's wing design compared to the baseline aircraft is the application of AAW technology, enabling the usage of high AR, thin and swept wing [19]. In contrast to the conventional wing design, the AAW technology integrates flight control design such that the entire wing acts as a control surface [18]. This leads to an improvement of aerodynamic drag, control power, and structural mass [19] [18]. In comparison to the conventional wing design the torsional stiffness is reduced and morphing leading and trailing edge control surfaces are applied to utilize the power of the air stream, which twists the wing to a favorable shape [18] [19]. The realization of this technology requires the assignment of a Digital Flight Control System (DFCS) for Horizon [20]. Successful flight research programs [19] [20] were conducted which facilitate the application of the AAW technology in the Horizon concept.

Several aeroelastic effects (e.g. flutter) have to be taken into account during the wing design. Especially flutter became an active constraint to the AAW design [18]. However, flight tests for a combat fighter proved, that the AAW can be designed with an acceptable flutter clearance [21]. Alternatively, the installed DFCS is able to ensure flutter suppression if an appropriate control system is included.

The integration of the AAW technology into the Horizon concept plane leads to an improvement in structural weight of the wing by approximately 5% to 20% [19], as well as the feasibility of using a high aspect ratio, thin, and swept wing. The high AR further decreases the induced drag and therefore improves the aerodynamic performance. As a first assumption the AR is chosen to be approximately 15 for calculating the energy enhancement potential.

With respect to the A320, the previous considerations for the AAW technology result in an improvement of the energy consumption by approximately 12%.

5.2.6 Flight Mechanical Stability

Regarding the stability of Horizon, one has to distinguish between flight phases with extended and retracted canard. Only in low speed flight phases like take-off, loiter, descent and landing the canard is extended to trim out the pitching moment of the main wing's high lift system. This technology was already applied in the Tupolev Tu-144 [25]. As seen in Figure 12, the canard can be designed in a way that the canard lift-coefficient is independent of the angle of attack. Hence the canard ensures the trimability of the aircraft in the lower speed ranges. In addition, the well natured stall behavior contributes to the aircraft's handling qualities and thus its controllability. Furthermore, it increases the lift when it is retracted.

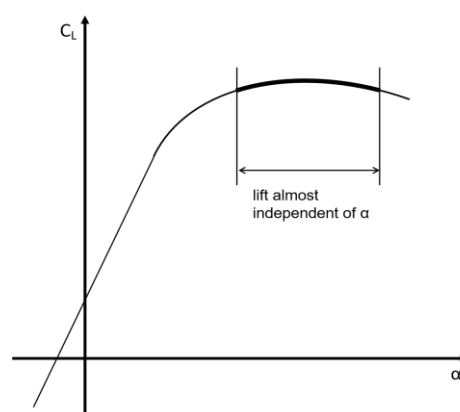


Figure 12 – Canard Lift over α [25]

Since the canard is retracted during cruise, Horizon's stability is affected. With this "flying wing" configuration it has to be ensured that flight mechanical stability is still maintained. Since a conventional wing is naturally unstable the developed aircraft is provided with an Active Stability Control System (ASCS). Such a system has been tested on the A340 in flight tests as well as in simulations [40]. Although this test aircraft is not tailless, it can be assumed, that in the next years the development of such systems becomes more successful and finally feasible. If it is necessary, a thrust vectoring system can be implemented as an option to ensure stability, since the X-31 was a successful program, where this technology was tested [41]. Yet, as described by Raymer [1] the

natural stability can be neglected as long as a suitable control system is used. Since the Horizon concept needs a DFCS for the AAW, the implementation of such an ASCS should not be a big issue. A further advantage for the DFCS is the shorter position range of the center of gravity due to Horizon’s fuselage and the favorable nose-up-pitching moment, as described in chapter 5.2.2.

5.2.7 Aerodynamic Design Summary

To summarize aerodynamic improvements, the Horizon concept is equipped with the following technologies:

- Laminar Flow Control over parts of the wing, vertical stabilizer and fuselage
- Boundary Layer Ingestion via aft-mounted engines
- Active Aeroelastic Wing
- Digital Flight Control System including an Active Stability Control system

In Table 10 the overall improvements by using the aerodynamic technologies are presented. All values must be seen as potential improvements with respect to the baseline aircraft. It has to be considered, that the reduction in wetted area cannot directly and simply be compared to the A320, since this reduction would lead to

Table 10 – Aerodynamic Technologies

Technology	Parameters	Improvement [%]
Reduced Wetted Area	$C_{D,min}$	28
LFC	$C_{D,min}$	21
	OEM ¹	-6.5
BLI	$C_{D,min}$	6
AAW	OEM	1.9
	Aspect Ratio	60

¹ without propulsion system mass

an overall change in the configuration and therefore a reduction in structural weight. It is rarely seen as a theoretical improvement in viscous drag by reducing the wetted area.

Finally, Figure 13 gives an overview over the particular technologies with their related energy improvements by using only one technology.

see important Note on Page 8

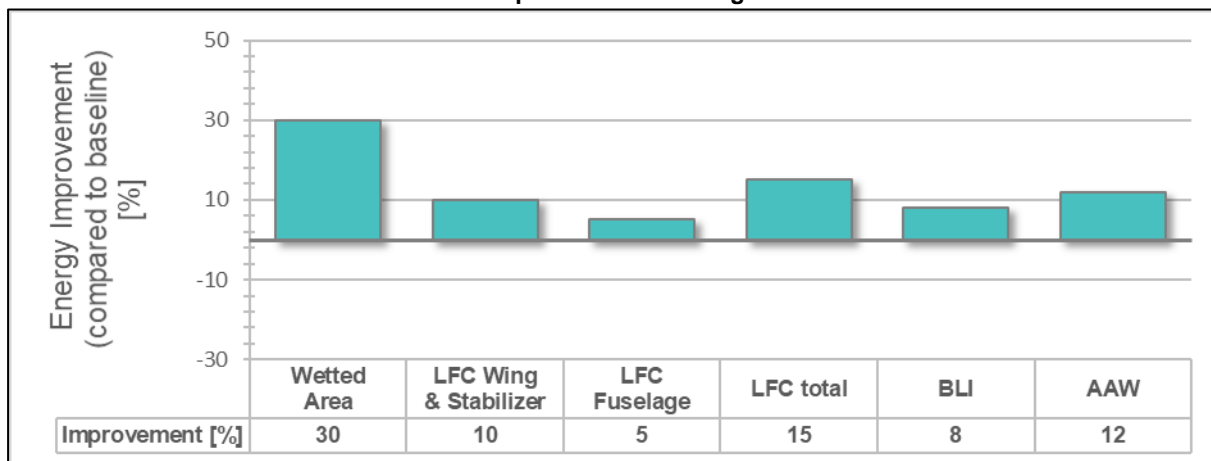


Figure 13 – Energy Improvements through Aerodynamic Technologies

5.3 Propulsion System Design

The proposed Horizon concept suggests a hybrid electric propulsion system consisting of two composite cycle engines (CCE), which are boosted by electric motors (see Figure 14). In the past, ETOPS (or EDTO) regulations have been gradually increased due to higher reliability of developed engines. For the sake of flight safety, a twin-engine configuration is recommended. For each propulsion device, the CCE as well as the EM provide shaft power. This power is fed into a gearbox which in turn drives the fan. The

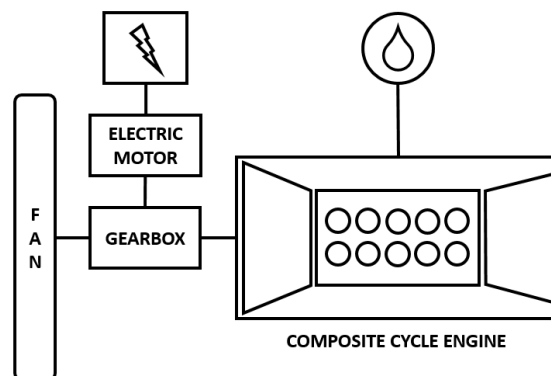


Figure 14 – Schematic Sketch of the Power Plant

described system is a parallel hybrid design, which enables an improvement of the propulsive efficiency [42]. Regarding rotational speed, a geared turbofan (GTF) has the advantage that the fan can be powered separately from the CCE. Due to the additional shaft power, the EM can intercept peaks in the performance requirements and thus the CCE can be designed for a relatively constant power level. The two electric boosted CCEs are partially embedded into the rear section of the Double Bubble fuselage. This design enables the previously mentioned BLI (see chapter 5.2.4) and results in a noise reduction due to the partially shielded inlet geometry.

5.3.1 Composite Cycle Engine

The CCE (see Figure 15) concept is not a completely new developed idea. Nevertheless, Bauhaus Luftfahrt e.V. investigated and recently released an own approach, which is used as basis for the Horizon power plant [24]. It features a conventional ICE implemented into an aircraft turbofan engine. The functional principle and the flow path between intake and nozzle are shown in Figure 16. The fan of the engine is, like in the final concept idea, a GTF. Studies have shown that already the GTF has the potential to reduce the SFC by up to 24% [44]. Nevertheless, with this design concept it is possible to keep the engine size at the same level compared to a similar normal turbofan engine, while an ultra-high bypass ratio (UBPR) can be realized. Due to this UBPR and a partially isochoric combustion of the ICE, a SFC reduction of 14.3% during take-off and 18.2% in climb can be achieved [24]. In addition to the SFC reduction, also the NO_x emissions were reduced by about 10% [24]. This is possible due to higher temperatures within, and lower temperatures at the exit of the combustion chamber. At the same time, peak pressures are raised and oxygen content is reduced.

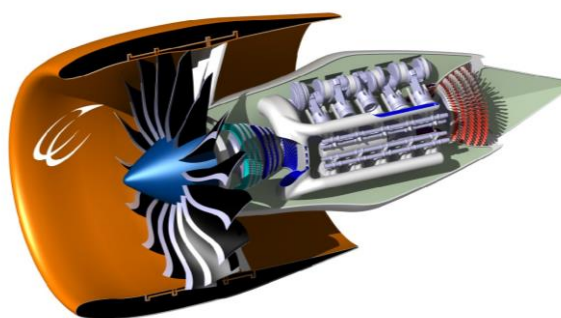


Figure 15 – Composite Cycle Engine [43]

This is possible due to higher temperatures within, and lower temperatures at the exit of the combustion chamber. At the same time, peak pressures are raised and oxygen content is reduced.

The drawback of the engine is the weight penalty. It is expected that the engine's weight is increased by 31% [24]. Due to alternative materials and their improved properties, this weight gain could be weakened. Using advanced materials for example, a reduction of nearly 30% of the mass of blades and vanes in the fan and compressor stage is possible (see chapter 5.1.3). Within the hot stages of the turbine, the mass of blades and vanes can even be reduced further by 65% [45] using ceramic matrix composites (CMC). It is also stated, that only due to the higher temperature resistance of CMCs, the SFC can be reduced up to 4.25% [46].

Blades and vanes have a significant weight influence on conventional turbofan engines. Unfortunately, this influence is reduced for the CCE, as the high-pressure turbine is replaced by a comparatively heavy ICE. However, a mass reduction of 5% is assumed, because alternative material's like CMCs are likely usable for the application on CCEs. There are also other suggestions for improvements, like intercoolers, which could further increase SFC savings and compensate the occurring weight penalties. Despite the low TRL of 2 [24], the individual components are well known and already designed. So, it is expected that the CCE can be taken into service in the targeted time frame [24].

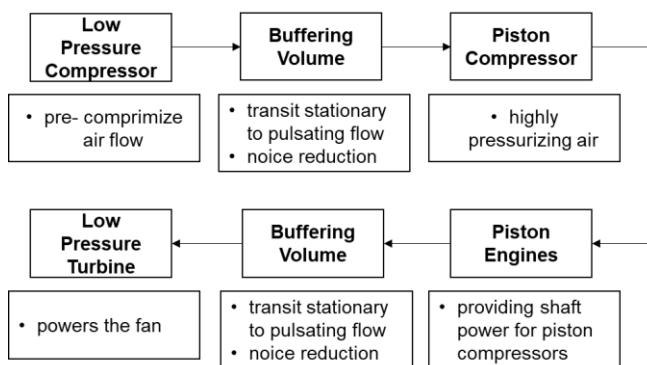


Figure 16 – Flow Path Between Intake and Nozzle

5.3.2 Fuel

The CCE is operated by an ICE, which runs on conventional Jet A-1 fuel. Even if other alternative fuels could find their application here, regular jet fuel is selected because it has a high mass specific energy with many years of research spent developing efficient engines [42]. This serves the main objective of this study, a reduction of the total energy consumption. Nevertheless, the use of other fuels like ethanol or liquefied petroleum gas, which is often unused in the industry and flared as waste, should at least be mentioned here. Their compatibility with ICEs is investigated more and more in recent researches [47] and could also be a possible solution.

5.3.3 Electrical Power System

The Horizon concept features an electric boosted engine for flight phases with high energy demand. Typical and already usable batteries like lithium-ion batteries offer a specific energy of approximately 250 to 300 Wh/kg [42, 48, 52], which is not sufficient for an electric or hybrid commercial passenger aircraft. However, there are several potential battery systems, currently being researched [53, 49], which might be used for the design. In this context, Table 11 contains an overview of three promising battery technologies. The magnesium-air battery seems to be the most appropriate choice due to the high theoretical specific energy and its economical and environmental properties. Unfortunately, the scientific research and estimations are still in the beginning [50]. On the other hand, lithium-based batteries, like lithium-sulfur and lithium-air batteries, are far more investigated and their technology is already at a high TRL. Because of the increasing demand and the research for batteries with high capacity, it is supposed that the specific energy of batteries will increase from 5% to 7% every year [42, 54]. Therefore, it is feasible that, in the year 2045, there will be batteries with a specific energy range of about 1000 to 1500 Wh/kg [42, 51, 52]. For this concept, lithium-sulfur batteries are selected, since it is probable that they will achieve the required specific energy and do not change their mass while discharging, like lithium-air batteries.

Table 11 – Battery Systems [48, 49, 44, 50, 51]

Battery Technology	Theoretical Specific Energy [Wh/kg]	Expected Specific Energy [Wh/kg]
Lithium - Sulphur	2570	500 – 1250
Lithium - Air	3500	800 – 1750
Magnesium - Air	3900	tbd

To state a reasonable decision for a possible specific energy, an investigation of the influence of the specific battery energy on the total energy consumption is offered in Figure 17. Based on this, Horizon's batteries are assumed to deliver a specific energy of 1000 Wh/kg, since further enhancements in battery specific energy are not as feasible as energy improvements resulting from the increase in the lower specific energy region.

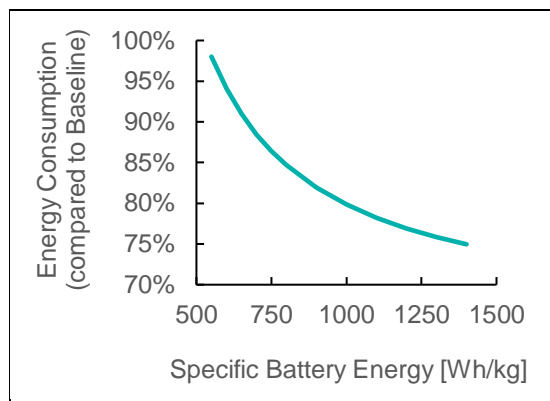


Figure 17 – Specific Battery Energy Sensitivity

As an additional assumption for the concept plane, the total battery mass includes extra batteries (10%) to consider unplanned flight situations (e.g. go-around). Moreover, an amount of 20% extra batteries is implemented, as the lifetime of a battery is tending to decrease (for example lithium-ion batteries [55]), if it is drained completely.

Besides the weight, also the required space is an important part of the sizing process. Lithium-air batteries in mean, have the highest density of the presented battery technologies with roughly 2310 kg/m³ [53, 56]. An estimation of the necessary battery installation space is provided in chapter 7.

The maximum charging rate is strongly influenced by the technical limitation of the battery itself. It is highly probable, that with only one single battery, the resulting charging time would highly exceed the favored turn-around time. Therefore, the installed batteries are split into 28 equally sized battery-packs, which can be charged separately. However, these split batteries entail an increased space demand, since the battery packs have to be installed in a safe and proper manner.

Due to the general progress in electric mobility, also the implementation of solar modules is discussed. The fundamental problem is the relatively low averaged solar irradiance of 340 W/m² [57]. The implementation of solar modules would not be worthwhile, even if the low efficiency of the solar modules is neglected, especially because a large amount of wetted area is required. With respect to the baseline aircraft (122 m² reference area), a 7h flight would only generate 0.69% of the 80 % reduced reference energy.

Horizon's electric motors are assumed to provide a specific power of 10 kW/kg [42]. A normal-conducting motor was selected to avoid several problems. First, a higher specific power requires a higher current, which leads to a reduction of the battery capacity (Peukert's law). Furthermore, high performance motors, like high-temperature superconducting motors, need cooling within the cryogenic temperature region increasing system complexity [58].

5.3.4 Propulsion System Design Summary

The previously mentioned technologies, implemented into the Horizon concept plane, have different influences on the aircraft performance parameters. A summary of these parameters is given in Table 12. In order to determine the influence on the energy consumption in detail, each

Table 12 – Propulsion Technologies

Technology	Parameters	Improvement [%]
Hybridization	Energy	20.2
GTF	SFC	22.1 ¹
CCE	SFC	18.2
	Engine Mass	-31
Advanced Materials	SFC	4.25
	Engine Mass	10

¹ The value is selected for the CCE [43] with the results of [44]

of these technologies is applied to the baseline aircraft and sized with the *PreHyST* tool. The impact of each technology on the energy consumption with respect to the baseline is shown in Figure 18.

see important Note on Page 8

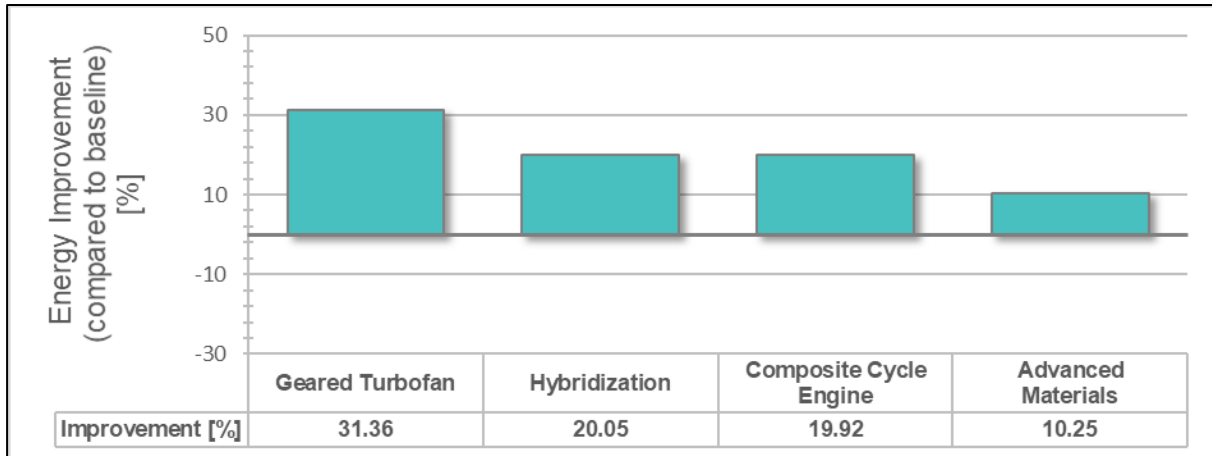


Figure 18 – Energy Improvements through Propulsion Technologies

5.4 Sizing Assumptions

In order to combine the presented technological improvements for the final sizing, certain restricting assumptions have to be made. This is necessary since the individual improvements that correspond to structural masses, parasitic drag and propulsive efficiency cannot simply be added up to one value. Therefore, rather conservative values are estimated by complying with the potential of the most influential technology that concerns each parameter to be enhanced.

In Figure 19 the unsized improvements in comparison to the baseline are showcased for all three categories. The contributors to all individual values are given in the Appendix.

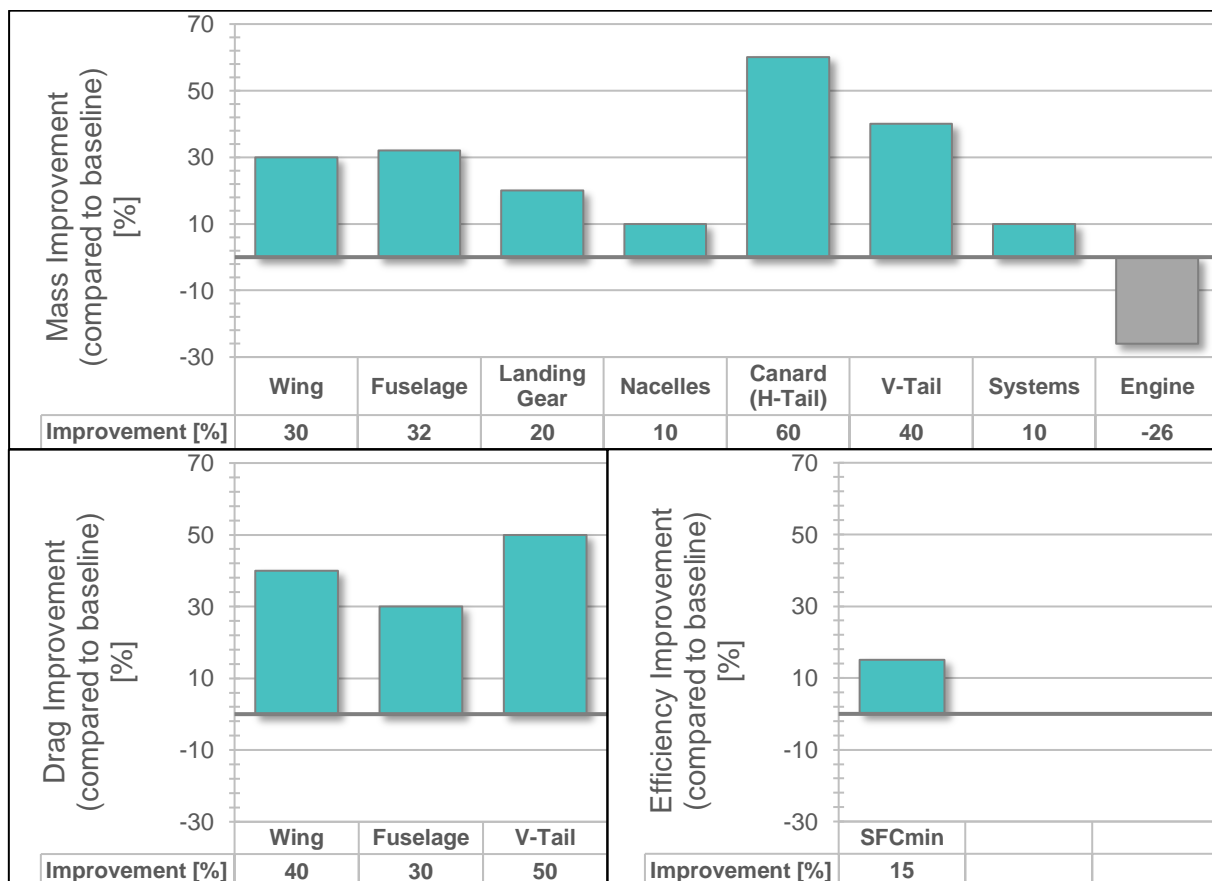


Figure 19 – Assumed Technological Improvement

6 Further Design Aspects

For the certification of the concept plane before EIS, the certification process must be slightly adapted to ensure the highest safety in regard to the implementation of the presented technologies. The major difference to existing aircraft is the introduction of a human autonomous autopilot (A/P). In this case, the commitment of a typical pilot is not necessary anymore, which additionally requires a fundamental change of the applicable certification specifications. The main task of this A/P is to regulate a highly safe and redundant working system, which is able to control the aircraft in every particular flight condition.

In general, the certification of new technologies and systems, as incorporated by Horizon, entails an extensive and long-lasting process, which could avoid their introduction to the market.

With steadily enhancement of numerical analysis methods, like CFD and FEM, the pace of investigation and evaluation of innovative technologies accelerates, while those methods get more and more accurate [46]. Even if flight tests and experiments are still mandatory today, it is probable that such numerical analysis can be treated as an alone standing prove for a technology to permit a safe and faster implementation into aviation.

Besides the certification of technical components, the safety during operation has to be ensured. Thereby, the evacuation plays a very important role. Horizon's fuselage offers two aisles and three doors on each side to allow for an evacuation within the time specified in the regulations.

The general operation of Horizon is possible with today's airport infrastructure, except for the electrical power supply for the installed battery-packs. Airports have to make sure to offer this power at every gate. Possible solutions are provided by the installation of underground cables or, for less frequented airports, energy providing airport vehicles. The required energy can be generated partly or completely by renewable energy sources like solar modules, wind power or geothermal energy.

To ensure an outstanding flight experience and a widespread customer acceptance, Horizon comes up with a cutting-edge friendly design. The wide Double Bubble fuselage provides the passenger with plenty of space to relax and to enjoy the flight.

The absence of a pilot is not a highly accepted idea nowadays, but with respect to the development of modern autonomic transport vehicles, the acceptance is expected to rise during the upcoming decades.

The influence of noise on passenger and airport environment is another factor that cannot be neglected when considering the acceptance of new aircraft designs and thus is also respected by NASA's N+ goals (see Table 1). The Horizon concept therefore involves hybrid-electric powered take-off and climb phases, in which lower rotational speeds for the CCEs occur. Consequently, noise can be reduced in those regions that are important in regard to certification and public interest. Another heavy contributor to airport noise is caused by unsteady airflows around extended high lift devices [59]. As the presented concept plane uses morphing leading and trailing edge control surfaces, coming along with the absence of gaps that lead to unsteady airflows, significant noise reductions can be expected.

The reduction of emissions is also a major aspect for future aircraft designs. Horizon's highly efficient CCEs are able to lower NO_x emission by about 10% [24]. The parallel hybrid layout of the propulsion system offers the possibility to operate the CCEs closer to their point of optimal efficiency, which decreases the fuel consumption and reduces emissions [4]. The cutting edge low drag design decreases propulsive power to an absolute minimum.

7 Horizon Concept Sizing

With respect to the assumptions made in chapter 5 concerning the implemented technologies, the concept plane can be sized to the TLARs constituted in chapter 3.1.

Similar to the resizing of the reference aircraft, the calculation of the optimum design point within the scope of a constraint analysis represents the first step of the initial sizing process of Horizon. However, there is no design rule for hybrid-electric aircraft specifying the location of the optimum design point, which is comparable to the design rule for conventional powered aircraft. In such, using the *PreHyST* tool, the whole design space is investigated to identify the design point and its degree of hybridization which includes the lowest total energy. The energy distribution in Horizon's design space, as well as the resulting optimum split point is illustrated in Figure 20. Note that the split point visualizes the installed hybridization of the developed aircraft as depicted in Figure 1 and described by Rings [4]. The design point is solely the projection of the split point to the highest constraint function.

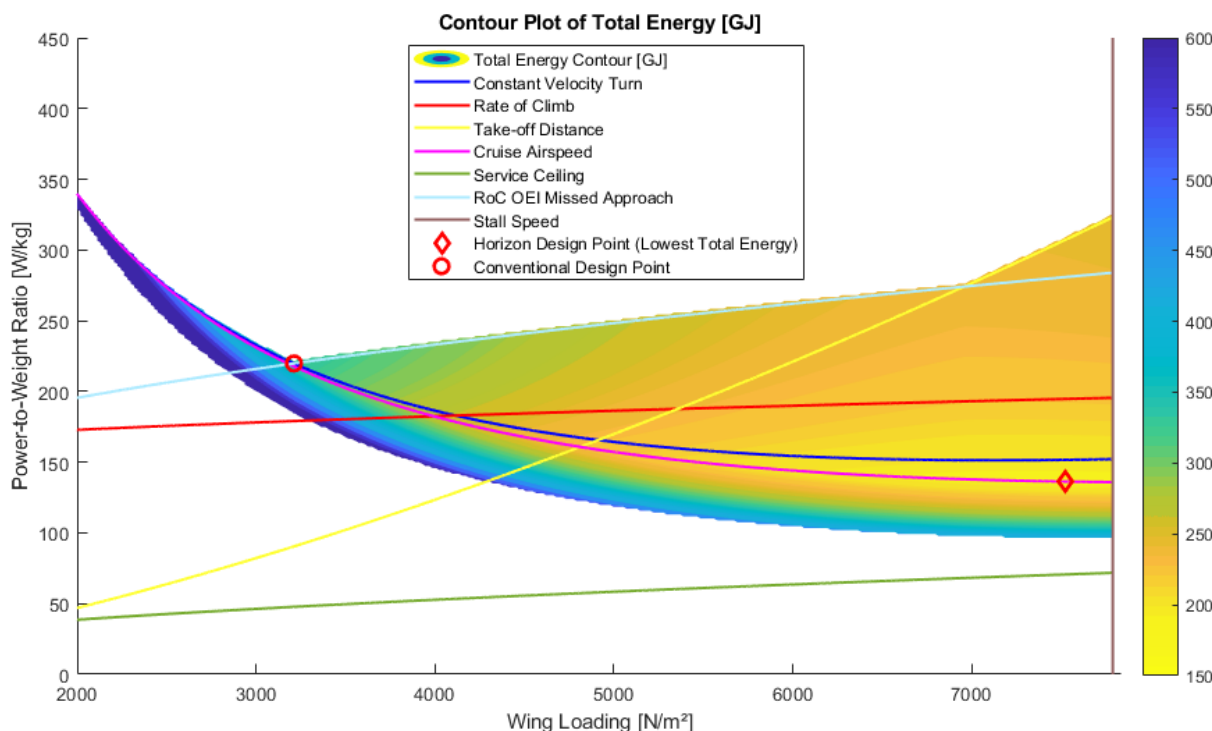


Figure 20 – Horizon Matching Diagram

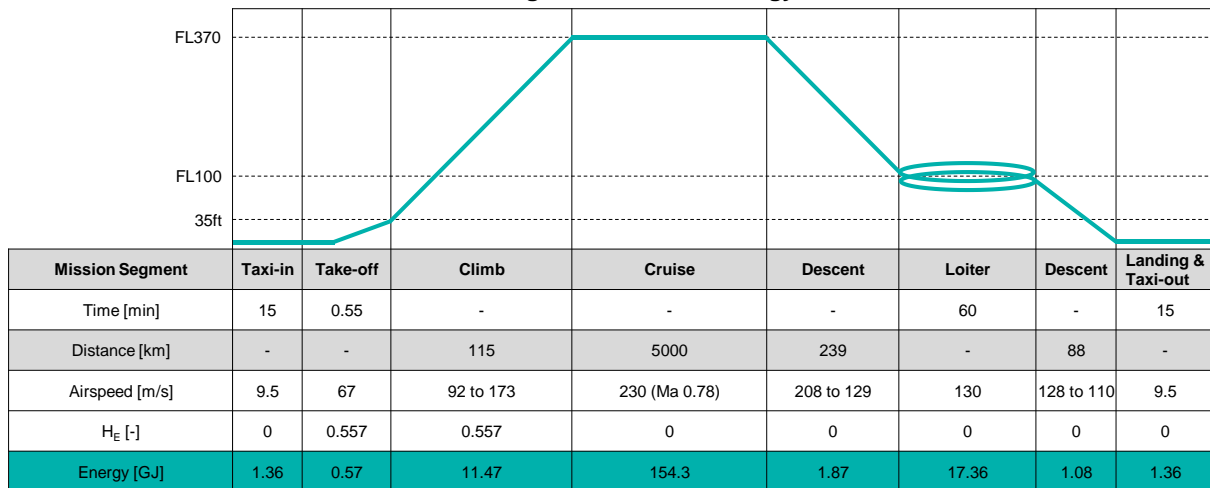
Horizon's design point is located at a power-to-weight ratio (P/W) of 307.3 W/kg and a W/S of 7525 N/m², while its split point is placed at a P/W of 136.3 W/kg. This results in an installed hybridization H_P of 55.7% and a design of the CCE to cruise conditions, as illustrated by the location of the split point on the cruise velocity constraint (see Figure 20). This split point indicates that 55.7% of the total propulsive power is provided by the EMs and 44.3 % is delivered by the CCEs. The mentioned hybridization is found to be optimal with respect to the design objective of the lowest total energy, since two major effects restrict higher (lower split point location) or lower (higher split point location) degrees of hybridization. On the one hand, a higher hybridization causes the use of battery power in cruise flight, in order to supply supporting EMs. This leads to a rapid increase of battery mass and total energy due to the specific energy of the installed batteries still being considerably lower than the appropriate value of kerosene [42]. On the other hand, a design of the CCEs to higher power demands than those appearing in cruise results in a suboptimal operation of the engines in cruise flight in terms of the SFC. This also entails an increase of total energy consumption and

MTOM. In contrast, the average SFC of the concept plane in cruise nearly equals the minimum SFC specified for the CCEs, as presented in Table 14.

For the design point outlined above, the mission analysis provides a MTOM of 36661 kg and a total energy use of 190.7 GJ, which leads to an overall improvement of the energy consumption by 74.9% in comparison to the A320. Therefore, the primary design target of reducing in flight energy consumption by at least 60% compared to the best in class aircraft of 2005 is entirely accomplished by the developed aircraft. Moreover, it nearly reaches the long-term objective of an 80% energy reduction. The energy distribution in the individual flight phases is diagrammed below. The degree of hybridization of energy (H_E) is pointed out for each phase, revealing the amount of energy taken from batteries.

$$H_{E,i} = \frac{\Delta E_{nc}}{\Delta E} \tag{3}$$

Table 13 – Horizon Flight Mission and Energy Distribution



Considering the calculated MTOM as well as the design and split point data, it can be shown that each CCE must deliver a power of 2.52 MW, while each EM of the parallel hybrid propulsion system has to provide a maximum power output of 3.17 MW. Regarding the assumption delineated in chapter 5.3.3, a total necessary battery installation space of 0.886 m³ is calculated and tripled to ensure a safe and proper battery arrangement. The exposed wing area is sized to a value of 47.8 m², resulting in a wing reference area of 75.2 m². For the same wing span in comparison to the reference aircraft (34.1 m), this leads to an AR of 15.46 for the introduced aircraft concept. As mentioned in chapter 5.2.6, the longitudinal instability of Horizon is compensated by a flight control system, so only sufficient control must be provided [1]. However, lateral stability still is assured by the application of a conventional vertical stabilizer. Based on the preliminary sizing results and by means of the method of tail volume coefficients [2], the area of the vertical stabilizer is estimated to 11.35 m².

The most important requirements and performance parameters, which are based on the assumptions made in chapter 5, are given in Table 14. It is shown that the TLARs conform to the most important requirements used for the A320. Additionally, the demands regarding the flapped lift coefficients for take-off and landing, as well as the clean lift coefficient remain unmodified. Yet, the maximum L/D changes, because the minimum parasitic drag coefficient can be reduced as specified in chapter 5.4.

According to chapter 5.3.1, the efficiency of the CCE is assumed to be increased by 15%, leading to a minimum BSFC of 169.2 g/kW/h. As the engine can operate nearly at its optimum condition during cruise flight, a very low fuel consumption can be achieved. However, the aircraft mass reduces during cruise, causing decreasing power demands and slightly more inefficient operation points of the CCE. Thus, the mean BSFC in cruise is found to be 174 g/kW/h.

With respect to these performance values, the energy carrier masses included in the developed aircraft are calculated. In combination with Horizon's structural masses and its propulsion system masses, a mass breakdown can be constituted (see Table 15). It has to be noted that the structural masses are determined by improving the structural masses of the baseline aircraft by the values given in chapter 5.4 and generating a new empty mass fraction for the concept plane. Thereafter, on the basis of the sizing, the masses of the particular structural components are computed with regard to the sized MTOM.

Table 14 – Horizon Requirements and Performance

Parameter	Unit	Value
TLARs		
Payload	kg	14250
Range	km	5000
Cruise Velocity	m/s	230
Cruise Altitude	m	11280
Service Ceiling	m	12130
Rate of Climb	m/s	12.2
Take-off Distance	m	2180
Landing Distance	m	1440
Aerodynamics		
$C_{L,max}$	-	1.50
$C_{L,max,TO}$	-	2.56
$C_{L,max,LD}$	-	3.00
$C_{D,min}$	-	0.01875
L/D_{max}	-	29
L/D_{cruise}	-	28.6
Propulsion System		
$BSFC_{min}$	g/kW/h	169.2
$BSFC_{cruise}$	g/kW/h	174

the masses of the particular structural components are computed with regard to the sized MTOM.

Table 15 – Horizon Mass Breakdown

Group	Mass [kg]	% MTOM	Group	Mass [kg]	% MTOM
Structures	8080	22.04	Systems and Equipment	3707	10.11
Wing	3042	8.30	Miscellaneous	2181	5.95
Canard	380	1.04			
Vertical Tail	164	0.45			
Fuselage	2610	7.12			
Landing Gear	1178	3.21			
Nacelles	706	1.93	Operating Empty Mass	15780	43.04
Propulsion	1812	4.94	Useful Load	20881	56.96
Engines	1155	3.15	Payload	14250	38.87
Engine Mounts	24	0.07	Fuel	4584	12.50
Electric Motors	633	1.73	Battery	2047	5.58
			Maximum Zero Fuel Mass	32077	87.50
			Maximum Take-off Mass	36661	100.00

8 Conclusion

To achieve the N+3 goal of a 60% to 80% reduction in total energy consumption, the focus during the conceptual design phase must be put on reductions in drag, mass and propulsive efficiency. During the development of Horizon, emphasis was laid on all aforementioned parameters and the following steps were successfully carried out:

1. Assessment of possible aircraft configurations
2. Deliberation of future technologies
3. Estimation of potential drag, mass and propulsive efficiency savings
4. Final sizing of the Horizon concept

The Horizon concept incorporates an optimized aircraft configuration with a variety of future technologies. The configuration emphasizes a Double Bubble fuselage, a retractable canard system, an Active Aeroelastic Wing and two hybrid composite cycle engines with an ultra-high bypass ratio. By applying innovative technologies like printed bionic structures, future materials as well as active Laminar Flow Control, significant energy savings can be achieved. In comparison to the Airbus A320-200 baseline aircraft, Horizon requires significantly less total mission energy with savings being as high as 74.9%.

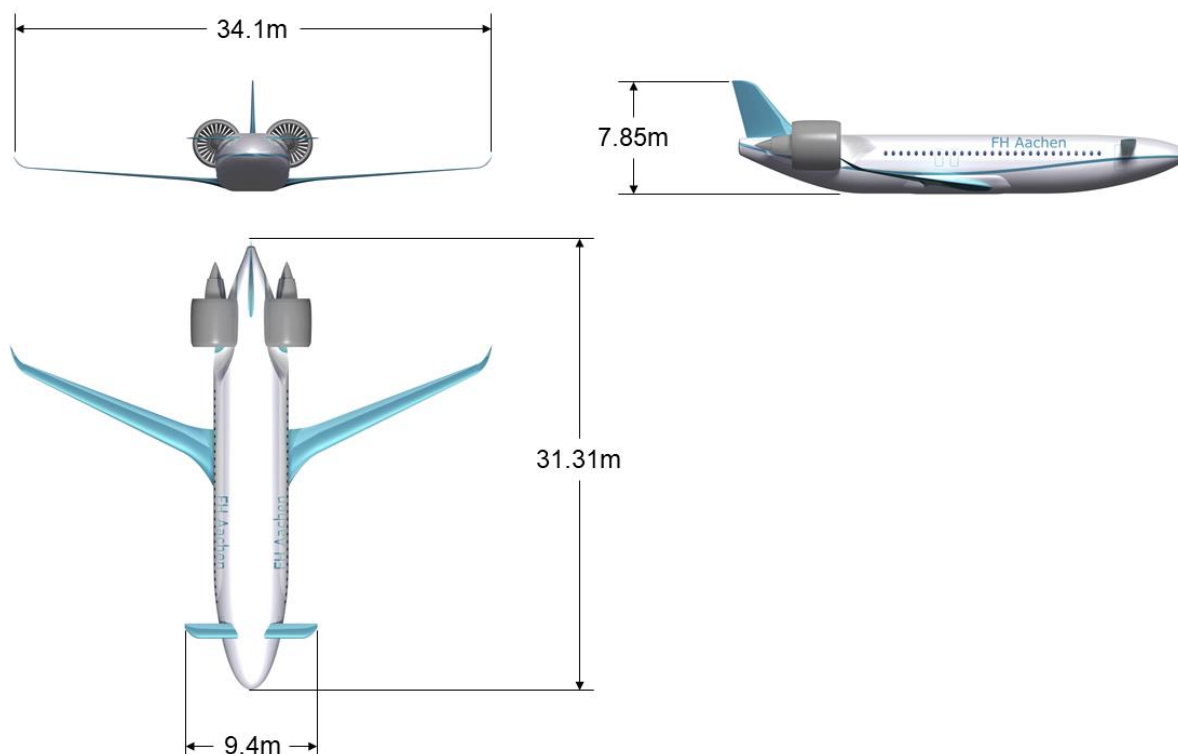


Figure 21 – Horizon Three-View

To achieve a design with an optimized feasibility, aspects like emissions, safety regulations and passenger acceptance were considered in the respective domains.

Within the 2045 timeframe, the Horizon concept promises a game-changing advance in the aerospace industry and offers an exciting new approach for future commercial aviation.

VII. Appendix

Appendix A – Contributors to Assumed Technological Improvements

Note: The presented values have to be understood in relation to chapter 5.4. The contributors to each group cannot simply be added up to one total value for the sizing. It is complied with the largest value of each group, while the influence of smaller contributors is lowered. This leads to a conservative estimation of the total influence.

Mass Improvement

Contributor	References	Improvement in 2045 [%]
<i>Wing</i>		
Active Aeroelastic Wing	[18, 19, 20, 21]	5 to 20
Single-Piece Design	[37]	10 to 30
Bionic Structures	[32]	20 to 30
Laminar Flow Control Pumps	[27]	-18
Decreased Area by 40%		-
Total		30
<i>Fuselage</i>		
Single-Piece Design	[37]	30
Bionic Structures	[32]	30
Future Materials	[33, 34, 35, 36]	30
Laminar Flow Control Pumps	[27]	-9
Total		32
<i>Landing Gear</i>		
Future Materials	[33, 34, 35, 36]	20
Total		20
<i>Nacelles</i>		
Future Materials	[33, 34, 35, 36]	20
Total		10
<i>Canard (Horizontal Tail)</i>		
Bionic Structures	[32]	20 to 30
Future Materials	[33, 34, 35, 36]	20
Decreased Area by 83%		-
Total		60
<i>Vertical Tail</i>		
Bionic Structures	[32]	20 to 30
Future Materials	[33, 34, 35, 36]	20
Laminar Flow Control Pumps	[27]	-18
Decreased Area by 40%		-
Total		40
<i>Systems</i>		
No Cockpit		10
Total		10
<i>Engine</i>		
Composite Cycle Engine	[24]	-31
Future Materials	[33, 34, 35, 36]	10
Total		-26

Parasitic Drag Improvement

Contributor	References	Improvement in 2045 [%]
<i>Wing</i>		
Laminar Flow Control	[27]	56
Total		40
<i>Fuselage</i>		
Laminar Flow Control	[27]	20
Boundary Layer Ingestion	[22]	26
Total		30
<i>Vertical Tail</i>		
Laminar Flow Control	[27]	56
Total		50

Propulsive Efficiency Improvement

Contributor	References	Improvement in 2045 [%]
<i>Minimal Specific Fuel Consumption</i>		
Composite Cycle Engine	[24]	18.2
Future Materials	[46]	4.25
Total		15

Appendix B – Horizon Impressions





VIII. References

- [1] D. P. Raymer, "Advanced Technology Subsonic Transport Study," National Aeronautics and Space Administration, Cleveland, Ohio, 2011.
- [2] D. P. Raymer, *Aircraft Design: A Conceptual Approach*, 5. ed., Reston, Virginia: AIAA, 2012.
- [3] S. Gudmundsson, *General Aviation Aircraft Design: Applied Methods and Procedures*, Oxford: Butterworth-Heinemann, 2014.
- [4] R. Rings, *Preliminary Sizing Studies of Light Aircraft with Parallel Hybrid Propulsion Systems*, Aachen: FH Aachen, 2018.
- [5] J. Ludowicy, *Preliminary Sizing Studies for Light Aircraft with Serial Hybrid Propulsion Systems*, Aachen: FH Aachen, 2018.
- [6] A. K. Kundu, *Aircraft Design*, Cambridge, New York: Cambridge University Press, 2010.
- [7] D. Hoak and D. Ellison, *The USAF Stability and Control DATCOM*, Wright-Patterson Air Force Base, Ohio: Air Force Flight Dynamics Lab, 1960.
- [8] P. Jenkinson, 2001. [Online]. Available: <http://booksite.elsevier.com/9780340741528/appendices/data-a/table-1/table.htm>. [Accessed 27 June 2018].
- [9] Airbus S.A.S., "Airbus A320 Aircraft Characteristics Airport and Maintenance Planning," Airbus S.A.S., Blagnac, Toulouse, 2005.
- [10] P. Jackson, *IHS Jane's All the World's Aircraft: Development & Production 2017-2018*, Coulsdon, Surrey: IHS Jane's, 2017.
- [11] J. Roskam, *Airplane Design Part I-VIII*, Kansas: Roskam Aviation and Engineering Corp., 1985.
- [12] [Online]. Available: <http://www.jet-engine.net/civtfspec.html>. [Accessed 27 June 2018].
- [13] L. J. Loftin, *Subsonic Aircraft: Evolution and the Matching of Size to Performance*, Hampton, Virginia: National Aeronautics and Space Administration, 1980.
- [14] C. Braun, *Aircraft Design 1, Lecture Notes Summer Term 2017*, Aachen: FH Aachen, 2017.
- [15] Aurora, *D8: Ultra-Efficient Commercial Aircraft - From the Jet Age to the Efficiency Age*, Aurora, 2016.
- [16] M. Drela, *Development of the D8 Transport Configuration*, Cambridge, Massachusetts: AIAA, 2011.
- [17] A. H. Bowers, O. J. Murillo, R. Jensen, B. Eslinger and C. Gelzer, "On Wings of the Minimum Induced Drag: Spanload Implications for Aircraft and Birds," National Aeronautics and Space Administration, Edwards, California, 2016.
- [18] P. M. Flick, M. H. Love and P. S. Zink, "The Impact of Active Aeroelastic Wing Technology on Conceptual Aircraft Design," in *Structural Aspects of Flexible Aircraft*.

- [19] E. W. Pendleton, D. Bessette, P. B. Field, G. D. Miller and K. E. Griffin, "Active Aeroelastic Wing Flight Research Program: Technical Program and Model Analytical Development," *Journal of Aircraft*, Vol. 37, No. 4, pp. 554-561, 2000.
- [20] E. Pendleton, P. Flick, D. Paul, D. Voracek, E. Reichenbach and K. Griffin, "The X-53 A Summary of the Active Aeroelastic Wing Flight Research Program," in *48th AIAA/ASME/ASCE/AHS/ASC Structures, Structural Dynamics, and Materials Conference, Structures, Structural Dynamics, and Materials and Co-located Conferences*, Honolulu, Hawaii, 2007.
- [21] D. Voracek, E. Pendleton, E. Reichenbach, K. Dr. Griffin and L. Welch, "The Active Aeroelastic Wing Phase I Flight Research Through January 2003," National Aeronautics and Space Administration, Edwards, California, 2003.
- [22] H.-J. Steiner, A. Seitz, K. Wieczorek, K. Plötner, A. T. Isikveren and M. Hornung, "Multi-Disciplinary Design and Feasibility Study of Distributed Propulsion Systems," 2012.
- [23] B. T. Blumentahl, A. A. Elmiligui, K. A. Geiselhart, R. L. Campbell, M. D. Maughmer and S. Schmitz, "Computational Investigation of a Boundary-Layer-Ingestion Propulsion System," *Journal of Aircraft*, Vol. 55, No. 3, pp. 1141-1153, 2018.
- [24] S. Kaiser, A. Seitz, S. Donnerhack and A. Lundbladh, "A Composite Cycle Engine Concept with Hecto-Pressure Ratio," pp. 9-11, July 2015.
- [25] P. Poisson-Quinton, "First Generation Supersonic Transports," in *The Princeton University Conference mtg No. 3-3 130 on the Future of Aeronautical Transportation*, Nov. 10-11, 1975.
- [26] Y. Gibbs, "NASA Armstrong Fact Sheet: Tu-144LL Supersonic Flying Laboratory," NASA, 28 February 2014. [Online]. Available: <https://www.nasa.gov/centers/armstrong/news/FactSheets/FS-062-DFRC.html>. [Accessed 27 June 2018].
- [27] N. Beck, T. Landa, A. Seitz, L. Boermans, Y. Liu and R. Radespiel, Drag Reduction by Laminar Flow Control, *Energies*, 2018, 11, 252.
- [28] J. Serpieri, "Cross-Flow Instability: Flow diagnostics and control of swept wing boundary layers," 2018.
- [29] B. Göksel and I. Rechenberg, "Active Flow Control by Surface Smooth Plasma Actuators," in *Rath HJ., Holze C., Heinemann HJ., Henke R., Hönlinger H. (eds) New Results in Numerical and Experimental Fluid Mechanics V. Notes on Numerical Fluid Mechanics and Multidisciplinary Design (NNFM), vol 92.*, Berlin, Heidelberg, Springer, 2006.
- [30] Z. Xin, H. Yong, W. Xunnian, W. Wanbo, T. Kun and L. Huaxing, "Turbulent boundary layer separation control using plasma actuator at Reynolds number 2000000," in *Chinese Journal of Aeronautics, Volume 29, Issue 5*, 2016, pp. 1237-1246.
- [31] G. Artana, J. D'Adamo, L. Léger, E. Moreau and G. Touchard, "Flow Control with Electrohydrodynamic Actuators," *AIAA Journal*, Vol. 40, No. 9, pp. 1773-1779, 2002.
- [32] G. Gardiner, "Bionic design: The future of lightweight structures," 8 11 2016. [Online]. Available: <https://www.compositesworld.com/blog/post/bionic-design-the-future-of-lightweight-structures>. [Accessed 15 6 2018].

- [33] R. S. Ruoff, D. Qian and W. K. Liu, Mechanical properties of carbon nanotubes: theoretical predictions and experimental measurements, Elsevier, 2003.
- [34] C. Soldano, A. Mahmood and E. Dujardin, Production, properties and potential of graphene, Toulouse, France: Elsevier, 2010.
- [35] L. Hall, "Nanotechnology Flight Test: Material Impact on the Future," NASA, 15 5 2017. [Online]. Available: <https://www.nasa.gov/feature/nanotechnology-flight-test-material-impact-on-the-future>. [Accessed 15 06 2018].
- [36] M. Mrazova, Advanced composite materials of the future in aerospace industry, Zilina, Slovak Republic: Incas Bulletin, 2013.
- [37] Dassault Aviation, Full Barell Composite - General Overview - Architecture, Concepts and Design Aspects, Vienna, Austria: Aeronautical Days 2006, 2006.
- [38] S. C. Rich, "Smithsonian.com," 16 08 2012. [Online]. Available: <https://www.smithsonianmag.com/arts-culture/aircraft-design-inspired-by-nature-and-enabled-by-tech-25222971/>. [Accessed 27 June 2018].
- [39] F. De Gregorio, D. Steiling, E. Benini and R. Ponza, "ERICA tiltrotor airframe wake characterization," 41st European Rotorcraft Forum 2015, 2015.
- [40] F. Sauvinet, "Longitudinal Active Stability: Key Issues For Future Large Transport Aircraft," in ICAS, 2000.
- [41] P. Huber and H. Schellenger, "X-31 Quasi-Tailless Flight Demonstration," in *NASA. Dryden Flight Research Center, Fourth High Alpha Conference, Volume 2; p. 14 p*, 1994.
- [42] H. Kuhn, A. Seitz, L. Lorenz, A. Isikveren and A. Sizmann, "Progress and Perspectives of Electric Air Transport," in *28th International Congress of the Aeronautical Sciences*, Brisbane, September 2012.
- [43] Bauhaus Luftfahrt e. V., "Composite Cycle Engine Concept - Technical data sheet," [Online]. Available: https://www.bauhaus-luftfahrt.net/fileadmin/user_upload/CCE_Data_Sheet.pdf. [Accessed 2018 06 17].
- [44] J. Bijewit, A. Seitz and M. Hornung, "Architectural comparison of advanced ultra-high bypass ratio turbofans for medium to long range application," in *Deutscher Luft- und Raumfahrtkongress*, 2014.
- [45] N. Takeshi, O. Takashi, I. Kuniyuki, S. Ken-ichi and I. Masato, "Development of CMC Turbine Parts for Aero Engines," *IHI Engineering Review*, vol. 47, no. 1, 2014.
- [46] S. W. Ashcraft, A. S. Padron, K. A. Pascioni and G. W. J. Stout, "Review of Propulsion Technologies for N+3 Subsonic Vehicle Concepts," National Aeronautics and Space Administration, Cleveland, Ohio, 2011.
- [47] Dr.-Ing. Benker et al., "Fortschrittliche alternative flüssige Brenn- und Kraftstoffe: Für Klimaschutz im globalen Rohstoffwandel," ProcessNet-Arbeitsausschuss „Alternative flüssige und gasförmige Kraft- und Brennstoffe“, 2017.
- [48] Martin Hepperle, "Electric Flight – Potential and Limitations," in *Energy Efficient Technologies and Concepts of Operation*, Lisbon, Portugal, 2012.

- [49] H. Zhang, X. Li and H. Zhang, "Li-S and Li-O₂ Batteries with High Specific Energy: Research and Development," 2017, p. 2.
- [50] F. Gebert, C.-S. Li, Y. Sun and S.-L. Chou, "Current Progress on Rechargeable Magnesium–Air Battery," p. 7, 2017.
- [51] J. Schömann, "Hybrid-Electric Propulsion Systems for Small Unmanned Aircraft," Technische Universität München, Doktorarbeit, 2014, p. 25.
- [52] A. Seitz, O. Schmitz, A. T. Isikveren and M. Hornung, "Electrically Powered Propulsion: Comparison and Contrast to Gas Turbines," 2012.
- [53] J. Christensen, P. Albertus, R. S. Sanchez-Carrera, T. Lohmann, B. Kozinsky, R. Liedtke, J. Ahmed and A. Kojica, "A Critical Review of Li/Air Batteries," *Journal of The Electrochemical Society*, pp. R1, R2, R21, 2012.
- [54] G. Warwick, "Electric Potential - Are battery technologies advancing fast enough to enable eVTOL," *Aviation Week & Space Technology*, pp. 38-41, 14 August 2017.
- [55] "Lithium Battery Failures," Woodbank Communications Ltd 2005, [Online]. Available: https://www.mpoweruk.com/lithium_failures.htm. [Accessed 27 June 2018].
- [56] Y. Ren, T. Zhao, P. Tan, Z. Wei and X. Zhou, "Modeling of an aprotic Li-O₂ battery incorporating multiple-step reactions," in *Applied Energy*, Hong Kong, China, Elsevier, 2017, p. 711.
- [57] NASA Earth Observatory, [Online]. Available: <https://earthobservatory.nasa.gov/Features/EnergyBalance/page2.php>. [Accessed 27 June 2018].
- [58] P. J. Masson, D. S. Soban, E. Upton, J. E. Pienkos and C. A. Luongo, "HTS Motors in Aircraft Propulsion: Design Considerations," *IEEE Transactions on Applied Superconductivity*, pp. 2218-2221, July 2005.
- [59] W. Graham, C. Hall and M. Vera Morales, "The potential of future aircraft technology for noise and pollutant emissions reduction," *Transport Policy*, pp. 36-51, 27 March 2014.

FH Aachen | Postfach 10 05 60 | 52005 Aachen

Dr. Johannes Hartmann

Dipl.-Ing. Til Pfeiffer

Deutsches Zentrum für Luft- und Raumfahrt (DLR)
Institut für Systemarchitekturen in der Luftfahrt |
Flugzeugentwurf & Systemintegration
Hein-Saß-Weg 22
21129 Hamburg

Attestation for Submission

Dear, Dr. Hartmann, dear Mr. Pfeiffer

The Department of Aerospace Engineering at FH Aachen – University of Applied Sciences hereby certifies that the report of the NASA/DLR Design challenge team has been approved and agreed with us. The related work has been developed and conducted by the student team without further support of our academic staff.

The submission to the NASA/DLR Design Challenge is supported.

Kind regards



Prof. Dr.-Ing. Carsten Braun

FH Aachen

Hohenstaufenallee 6
52064 Aachen
Deutschland
www.fh-aachen.de

**Prof. Dr.-Ing
Carsten Braun**

**Fakultät für
Luft- und Raumfahrttechnik**

**Lehr- und Forschungsgebiet
Luftfahrzeugtechnik**

Kontakt

T +49. 241. 6009 52374
F +49. 241. 6009 52680
c.braun@fh-aachen.de

Datum

29.06.2018